

The phenylpropanoid pathway inhibitor piperonylic acid induces broad-spectrum pest and disease resistance in plants

Willem Desmedt¹, Wim Jonckheere¹, Viet Ha Nguyen¹, Maarten Ameye¹, Noemi De Zutter¹, Karen De Kock¹, Jane Debode², Thomas van Leeuwen³, Kris Audenaert¹, Bartel Vanholme¹, and Tina Kyndt¹

¹Ghent University

²ILVO

³Affiliation not available

April 30, 2021

Abstract

While many phenylpropanoid pathway-derived molecules act as physical and chemical barriers to pests and pathogens, comparatively little is known about their role in regulating plant immunity. To explore this research field, we transiently perturbed the phenylpropanoid pathway through application of the CINNAMIC ACID-4-HYDROXYLASE (C4H) inhibitor piperonylic acid (PA). Using bioassays involving diverse pests and pathogens, we show that transient C4H inhibition triggers systemic, broad-spectrum resistance in higher plant without affecting growth. PA treatment enhances tomato (*Solanum lycopersicum*) resistance in field and laboratory conditions, thereby illustrating the potential of phenylpropanoid pathway perturbation in crop protection. At the molecular level, transcriptome and metabolome analyses reveal that transient C4H inhibition in tomato reprograms phenylpropanoid and flavonoid metabolism, systemically induces immune signaling and pathogenesis-related genes, and locally affects reactive oxygen species metabolism. Furthermore, C4H inhibition primes cell wall modification and phenolic compound accumulation in response to root-knot nematode infection. Although PA treatment induces local accumulation of the phytohormone salicylic acid, the PA resistance phenotype is preserved in tomato plants expressing the salicylic acid-degrading NahG construct. Together, our results demonstrate that transient phenylpropanoid pathway perturbation is a conserved inducer of plant resistance and thus highlight the crucial regulatory role of this pathway in plant immunity.

Introduction

Induced resistance (IR) refers to a phenotypic state in which an exogenous stimulus conditions the plant for reduced susceptibility to future biotic challenges (De Kesel *et al.* 2021). IR stimuli include chemical compounds, beneficial microbes and various (a)biotic stresses (Conrath *et al.* 2006; Martínez-Medina *et al.* 2016; Mauch-Mani, Baccelli, Luna & Flors 2017). Once triggered, IR is memorized through long-term epigenetic, proteomic and metabolic alterations (Balmer, Pastor, Gamir, Flors & Mauch-Mani 2015; Conrath, Beckers, Langenbach & Jaskiewicz 2015) and may last the plant's entire life cycle (Conrath *et al.* 2015).

IR has been successfully used in crop protection (Walters & Fountaine 2009), and several IR-inducers are available commercially. Examples include beneficial microbes such as *Trichoderma* spp. (Perazzolli, Roatti, Bozza & Pertot 2011; Martínez-Medina *et al.* 2017), functional analogs of the defense hormone salicylic acid (SA) such as acibenzolar-S-methyl (Romero, Kousik & Ritchie 2001) or probenazole (Yoshioka, Nakashita, Klessig & Yamaguchi 2001), as well as oligosaccharide-based products such as COS-OGA, a combination of chito-oligosaccharides and oligogalacturonides (van Aubel, Buonatesta & Van Cutsem 2014; van Aubel, Cambier, Dieu & Van Cutsem 2016).

IR involves both direct activation of plant defense mechanisms and priming, enhanced induction of defense responses upon later challenge (Mauch-Mani *et al.* 2017; De Kesel *et al.* 2021). Examples of defense mechanisms involved in IR include accumulation of proteins with anti-pathogen activity (van Loon, Rep & Pieterse 2006), production of phytoalexins (Ahuja, Kissen & Bones 2012; Desmedt, Mangelinckx, Kyndt & Vanholme 2020) and cell wall reinforcement (Luna *et al.* 2011; Malinovsky, Fangel & Willats 2014; Veronico *et al.* 2018).

Both defense metabolite accumulation and cell wall reinforcement depend at least partially on the phenylpropanoid pathway (PPP) (Dixon *et al.* 2002; La Camera *et al.* 2004; Miedes, Vanholme, Boerjan & Molina 2014). In this pathway, phenylalanine is deaminated by PHENYLALANINE AMMONIA LYASE (PAL) to *trans*-cinnamic acid, which is *para*-hydroxylated by CINNAMIC ACID-4-HYDROXYLASE (C4H) to *para*-coumaric acid. *Para*-Coumaric acid is activated by 4-COUMAROYL-CoA-LIGASE to form *para*-coumaroyl-CoA, a reactive intermediary in the biosynthesis of lignin monomers and numerous other PPP-derived metabolites (Vogt 2010). Several phenylpropanoids are phytoanticipins or phytoalexins in their own right, as are numerous PPP-derived metabolites such as flavonoids, coumarins, stilbenoids and diarylheptanoids (Mathesius 2018; Desmedt *et al.* 2020). Finally, the PPP is also, together with the shikimate pathway, involved in SA biosynthesis (Dempsey, Vlot, Wildermuth & Klessig 2011).

Given the PPP's diverse roles in plant defense, one might expect PPP inhibition to impair plant immunity. Chemical or genetic PAL inhibition is indeed associated with increased susceptibility in various pathosystems, and high basal or induced PAL activity is often positively correlated with resistance (Wang, Wang & Ning 2019; Yadav *et al.* 2020). Downstream of the core PPP, stress-induced lignification and accumulation of PPP-derived phytoalexins are common resistance mechanisms (Dixon *et al.* 2002; Obermeier *et al.* 2013; Chezem, Memon, Li, Weng & Clay 2017; Veronico *et al.* 2018; Ranjan *et al.* 2019; Lee *et al.* 2019; Desmedt *et al.* 2020). Accordingly, it seems logical that C4H inhibition would also reduce disease resistance. However, Schoch and colleagues hinted that the opposite might be true by showing that co-application of piperonylic acid (PA), a C4H inhibitor (Schalk *et al.* 1998), and β -megaspermin, a *Phytophthora megasperma* elicitor protein, to tobacco BY-2 cells dramatically increased SA accumulation – something not seen when PA or β -megaspermin were applied individually (Schoch, Nikov, Alworth & Werck-Reichhart 2002). This led the authors to suggest that SA accumulation after combined PA and β -megaspermin elicitation might induce SA-dependent defense responses (Schoch *et al.* 2002). However, the hypothesis that PA might induce plant resistance has, to the best of our knowledge, never been tested.

We investigated if and how PA induces plant resistance by performing bioassays with various pathogens and pests, transcriptome and metabolome analysis, RT-qPCR and biochemical assays. As a model plant, we focused on tomato, which is the world's most widely consumed horticultural crop and is susceptible to numerous agriculturally important pests and diseases (Gould 1992; Blancard 2013).

Materials and methods

Plant material

Tomato (*Solanum lycopersicum* L. 'Moneymaker') seeds were germinated in potting soil in a growth chamber (24°C, 12/12 light/dark). Five days after emergence, seedlings were transplanted to pots containing a 3:1 (v/v) mixture of sand and sieved potting soil (Structural Type 1, Snebbout). Seedlings were watered three times a week and fertilized weekly with 30 ml of fertilizer (Soluplant NPK 19-8-16+4MgO+ME, Haifa Chemicals, 1 g l⁻¹). Rice (*Oryza sativa* L. 'Nipponbare') seeds (GSOR-100, USDA) were grown as in Nahar *et al.* (2011).

Chemical treatments

Piperonylic acid (PA; Sigma-Aldrich, catalog nr. P49805) was prepared as a 100 mM stock solution in dimethyl sulfoxide (DMSO; Duchefa Biochemie), diluted with distilled water and amended with 0.1% (v/v) Tween 20 (Sigma-Aldrich). Mock treatments consisted of distilled water with the same concentrations of Tween 20 and DMSO. Plants were sprayed with an atomizer until thoroughly wetted. Unless otherwise mentioned, PA was applied twice (8 and 1 days before inoculation) at a concentration of 300 μ M.

Tomato bioassays with pathogens and pests

Tomato seedlings were inoculated two weeks after transfer (24 h after second PA treatment) with 250 *Meloidogyne incognita* second-stage juveniles (J2s), unless otherwise mentioned. Roots were collected 28 days after inoculation (dai), washed and stained with 1:8-diluted Alcoferm Raspberry Red dye. After destaining in acidified glycerol, galls were counted under a stereo microscope. Rice - *Meloidogyne graminicola* assays were performed similarly, but plants were harvested 14 dai. N = 8, repeated at least twice.

Pseudomonas syringae DC3000 was grown on King's B agar with 75 mg l⁻¹ rifampicin and transferred to liquid King's B (without rifampicin, 28°C). Cells were centrifuged, resuspended in 10 mM MgSO₄ (OD₆₀₀ = 0.15) and amended with 0.05% (v/v) Silwet 77. Tomato seedlings (two fully expanded leaves, 24 h after second PA treatment) were then dipped in the bacterial suspension. Seedlings were kept at 100% relative humidity (RH) 24 h before and after dip-inoculation. Five dai, leaves were detached and photographed and the number of visible specks per cm² of leaf area was counted. N = 12, repeated twice.

Bioassays with *Botrytis cinerea* R16 (Faretra & Pollastro 1991) were performed as in Audenaert *et al.* (2002) using tomato leaves from four-week old plants detached 24 h after the second PA treatment. Four dai, disease progression was monitored in a phenotyping robot as in Meng *et al.* (2020). N = 8 (8 plants, 32 leaflets), repeated twice.

Aculops lycopersici was cultured on tomato (*S. lycopersicum* 'Moneymaker', 28°C, 50% RH, 16:8 light/dark). Thirty adults were transferred to a 1 cm-diameter tomato leaf disk, which was placed on the second leaf of a tomato seedling (24 h after second PA treatment). Ten dai, mites were counted under a stereo microscope. N = 6, repeated twice.

Tetranychus urticae (London strain, tomato-adapted (Wybouwet *et al.* 2015)) was expanded on common bean (*Phaseolus vulgaris* L. 'Prelude'). Ten adult females were transferred to tomato plants (*S. lycopersicum* 'Moneymaker', 28°C, 50% RH, 16:8 light/dark) 24 h after second PA treatment, and ten dai offspring (mobile stages) were counted under a stereo microscope. N = 8, repeated twice.

Frankliniella occidentalis was reared on bean pods (28°C, 70% relative humidity, 14:10 light/dark). Ten synchronized adult females were transferred to three-week-old tomato seedlings (*S. lycopersicum* 'Moneymaker') in ventilated Plexiglass cylinders (90 x 35 mm). Thrips could oviposit for 24 h, after which they were removed. Only plants from which all ten adults could be recovered were retained. Four days after adult removal, offspring were counted under a stereo microscope. N = 15, repeated twice.

Field trial with root-knot nematodes

A Good Experimental Practice-compliant trial was performed between September 2019 and February 2020 in a naturally nematode-infested greenhouse in Ispica (Sicily, Italy; coordinates 36.723783°N 14.968736°E) by SATA s.r.l (Quargernata, Italy). Treatments were arranged in a randomized complete block design with four 22 m² plots per treatment (22 tomato plants per plot, *S. lycopersicum* 'Ciringuito F1', planted September 9th 2019). The pre-trial nematode population was assessed as in Hallmann & Viaene (2013). PA was applied using a handheld sprayer (300 µM PA, 0.1% (v/v) DMSO and 0.1% (v/v) Tween 20) three times: eight and one days before transplanting and two weeks after transplanting. The nematicide Cedroz (Eastman), containing geraniol (121 g l⁻¹) and thymol (41 g l⁻¹), was used as a reference treatment and was applied per the manufacturer's guidelines (9 l ha⁻¹ total, 6 fortnightly applications). Starting in October 2019, four (intermediate assessments) or ten (final assessment) tomato plants per plot were uprooted and evaluated for vigor, phytotoxicity and galling severity on the Zeck scale (Zeck 1971). Yield was evaluated by picking and weighing ripe fruits weekly between December 2019 and February 2019.

Evaluation of acute toxicity of piperonylic acid

Acute toxicity of PA to *M. incognita* was evaluated by incubating 50 J2s in 300 µM PA or a corresponding mock solution and assessing motility after 48 h. PA's acute toxicity to *P. syringae* DC3000 and *B. cinerea* R16 was tested by adding 300 µM PA to their media and monitoring growth (OD₆₀₀ after 24 h for *P.*

syringae and colony area after five days for *B. cinerea*). Acute toxicity to *T. urticae*, *A. lycopersici* and *F. occidentalis* was tested as by Xue *et al.* (2020). Briefly, ± 25 adults (*T. urticae*, *A. lycopersici*) or larvae (*F. occidentalis*) were placed on 1 cm² leaf discs and sprayed with 300 μ M PA or a mock solution in a spray tower; mortality was recorded after three days.

Biochemical assays for phenylpropanoid pathway activity

Tomato roots, stems and leaves were harvested seven days with 400M. *incognita* J2s (three weeks after transplantation). Stem samples consisted of the stem section between roots and cotyledons, leaf samples of the first, second and third leaves and root samples of the whole root system. Samples were ground in a liquid nitrogen-chilled mortar. Lignin and phenolic compound quantification were repeated three times, using five biological replicates per treatment (consisting of 2-3 pooled seedlings).

Lignin was quantified using the acetyl bromide assay. Cell walls were prepared as in Van Acker *et al.* (2013), and the resulting extract was dried in a fume hood, weighed and suspended in 300 μ l 25% acetyl bromide (Sigma-Aldrich). After two hours incubation (50°C, 800 rpm), samples were placed on ice and diluted with 1.5 ml acetic acid. After centrifugation (10 minutes, 19 330g, RT), 300 μ l supernatant was mixed with equal volumes 2M NaOH and 0.5M hydroxylamine (Sigma-Aldrich) and centrifuged (10 minutes, 19 330g, RT). Absorbance at 280 nm was measured in a microplate reader (Tecan Infinite F200 Pro) and lignin content was calculated according to Barnes & Anderson (2017). Because no extinction coefficient for tomato lignin was available, that of *A. thaliana* reported by Xue *et al.* (2008) was used.

Free and cell-wall bound phenolic compounds were quantified using the Folin-Ciocalteu assay (Ainsworth & Gillespie 2007). Free phenolics were extracted from ± 100 mg tissue with 20 μ l mg⁻¹ 80% (v/v) ethanol (30 minutes, RT). After centrifugation (5 minutes, 19 330g, RT), 125 μ l supernatant was mixed with 675 μ l distilled water, 37.5 μ l Folin-Ciocalteu reagent (Sigma-Aldrich) and 375 μ l 20% (w/v) Na₂CO₃. After 15 minutes, absorbance at 765 nm was measured in a spectrophotometer (VWR UV1600PC) and phenolic compound concentration was calculated using a gallic acid standard curve.

The residue left after ethanol extraction was washed with 80% ethanol and extracted overnight with 20 μ l mg⁻¹ 1M NaOH to release cell wall-bound phenolic compounds. After centrifugation (5 minutes, 19 330g, RT), 125 μ l NaOH extract was mixed with 1.05 ml distilled water and 37.5 μ l Folin-Ciocalteu reagent and absorbance was measured as for free phenolic compounds.

3,3-diaminobenzidine (DAB) staining

Second leaves of three-week-old tomato plants were detached, petioles were wrapped in wet tissue paper and leaves were placed on petri dishes in trays filled with water with only the petiole touching the water. After 24 h in an incubator (24°C, 16:8 light/dark), each leaflet was treated by applying three 20 μ l droplets of 300 μ M PA solution, three 20 μ l droplets of mock solution or wounding with a scalpel (positive control). Leaflets were sampled 1, 3, 6 and 24 h post treatment and DAB-stained as in Daudi & O'Brien (2012). Four leaves (16 leaflets) were used per treatment and time point, and the experiment was repeated twice.

Guaiacol peroxidase assay

Guaiacol peroxidase activity was quantified as in MacAdam *et al.* (1992). Roots and shoots (from cotyledons upwards) of tomato seedlings were flash-frozen in liquid nitrogen 14 days after transplantation (24 h after second PA treatment) and ground in a liquid nitrogen-chilled mortar. ± 75 mg powder was extracted with 8 μ l mg⁻¹ cold extraction buffer (0.8 M KCl and 8 g l⁻¹ polyvinylpyrrolidone in 50 mM potassium phosphate buffer, pH 6.0). After centrifugation (10 minutes, 19 330g, 4°C), 10 μ l extract was mixed with 990 μ l assay buffer (3.3 mM guaiacol and 0.4 mM H₂O₂ in 100 mM potassium phosphate buffer, pH 6.0). Absorbance increase at 436 nm was recorded every 15 seconds for 3 minutes. Six biological replicates were used per treatment (each consisting of 2-3 pooled seedlings) and the experiment was repeated twice. The slope of the resulting curve was used as a measure of guaiacol peroxidase activity.

Untargeted metabolomic profiling and phytohormone analysis

Tomato seedlings were flash-frozen in liquid nitrogen fourteen days after transplantation (24 h after the second PA treatment). Roots and shoots (from cotyledons upwards) were ground in a liquid-nitrogen chilled mortar. Six samples (3 plants per sample) were analyzed per treatment. 100 mg powder was extracted with 2 ml cold methanol (30 minutes, 1000 rpm, 25°C) and centrifuged (10 minutes, 19 330g, RT). The supernatant was dried in a vacuum concentrator (Labconco CentriVap) at 35°C, while the residue was air-dried (24 h, 60°C) and weighed. Metabolites were dissolved in 200 µl 1:1 miliQ-water-cyclohexane (15 minutes, 1200 rpm, RT) and centrifuged (5 minutes, 19 330g, RT).

Seventy µl aqueous phase was filtered through a 0.2 µm filter (PAL AcroPrep) and 3 µl filtrate was analyzed by reversed-phase UPLC (Acquity UPLC I-class, Waters) coupled to a quadrupole-time-of-flight mass spectrometer (Vion IMS QToF, Waters) via an electrospray ionization source in negative ionization mode. Chromatography and MS conditions were as in De Meester et al. (2018). Pooled control samples, prepared by combining 3 µl of each sample, were used for chromatogram alignment and quality control.

Data were normalized to sample dry weight, and features were filtered using three criteria: (a) non-zero intensity in all replicates of at least one treatment, (b) mean MS intensity > 5 in at least one treatment and (c) relative SD < 30% in pooled control samples. Features were quantile-normalized (Bolstad, Irizarry, Åstrand & Speed 2003), centered and generalized logarithm-transformed (Durbin, Hardin, Hawkins & Rocke 2002) using MetaboAnalyst v. 5.0 (Chong, Wishart & Xia 2019). Differentially abundant features were identified using FDR-adjusted heteroscedastic t-tests with a significance threshold of $P < 0.05$ and absolute \log_2 -fold change > 1. Pathway analysis was performed using Mummichog v. 2.0 (Li *et al.* 2013) as implemented in MetaboAnalyst v. 5.0, with following parameters: mass tolerance 5.0 ppm, retention time included, primary ions enforced, P-value cut-off 0.05, *A. thaliana* pathway library.

For the targeted quantification of phytohormones, plant material was collected in the same manner as for metabolome profiling and 100 mg of this material was used for analysis using the methodology and instrumentation described in (Haeck et al. 2018).

Nematicidal assay on extracts from PA-treated plants

Extracts for nematicidal assays were prepared in the same manner as for UPLC-MS/MS profiling. Briefly, ground tissue was extracted with 5 ml methanol g^{-1} tissue (30 minutes, RT), after which the extract was filtered, dried in a rotary evaporator (35°C), dissolved in 0.5 ml water g^{-1} tissue and defatted with cyclohexane. A two-fold dilution series (from 2:1 to 1:8 mass-to-solvent ratio) was prepared, and ± 100 *M. incognita* J2s were incubated in 600 µl diluted extract. Nematode motility was evaluated after 4, 24 and 48 h. Four biological replicates, each consisting of 5-6 tomato plants, were used per treatment.

Gene expression analysis

Roots and shoots (from cotyledons upwards) were collected for mRNA sequencing 14 days after transplantation (one day after second PA treatment). For RT-qPCR, roots and shoots were harvested 6, 24 and 72 h after the second PA treatment. Samples were ground in a liquid-nitrogen chilled mortar.

For mRNA sequencing, RNA was extracted from ± 100 mg ground tissue (Quick-RNA Plant Miniprep Kit, Zymo Research). Three biological replicates, each consisting of four pooled plants, were used per treatment. Library preparation, sequencing and data analysis were as in (Ghaemi *et al.* 2020). Briefly, libraries were prepared using the QuantSeq 3' mRNA-Seq library prep kit (Lexogen), library quality was verified using an Agilent Bioanalyzer 2100 and libraries were sequenced on an Illumina NextSeq 500 platform. Data quality was assessed using FastQC (Andrews 2010), reads were trimmed with Trimmomatic (Bolger, Lohse & Usadel 2014; 5 bp sliding window, bases with Phred scores < 20 were trimmed and reads < 40 bp were removed). Trimmed reads were mapped to the tomato reference genome (ITAG 4.0, Hosmani *et al.* 2019) using STAR (Dobin & Gingeras 2015) and reads were counted using the *summarizeOverlaps* function of the *RGenomicAlignments* package (Lawrence *et al.* 2013). Differentially expressed genes were identified using the *R DeSeq2* package (Love, Huber & Anders 2014). Genes were considered differentially expressed if FDR-adjusted $P < 0.05$ and $|\log_2 FC| > 0.7$. PLAZA 4.5 (Van Bel *et al.* 2018) was used for gene ontology analysis.

For RT-qPCR, RNA was extracted from ± 100 mg ground tissue (RNEasy Plant kit, Qiagen,), DNase-treated (DNase I, Thermo Fisher Scientific) and converted to cDNA (Tetro cDNA synthesis kit, Bioline). RT-qPCR conditions were as in De Kesel *et al.* (2020). Primer sequences are listed in **Supplementary Table S1** . Three reference genes were used, using primer sequences obtained from Cheng *et al.* (2017). Reference gene stability in shoot and root was verified using our mRNA-seq dataset. Amplification efficiency and relative expression were calculated using LinRegPCR v. 2020.0 (Ruijter *et al.* 2009). Statistical significance was determined using FDR-adjusted t-tests. Four biological replicates, consisting of 2-3 pooled plants, were used per treatment.

Statistical analysis

Statistical analyses were performed in R (v. 4.0.0). For bioassays, generalized linear models were fitted (binomial for binary variables, negative binomial for count data and Gaussian for continuous variables) and model assumptions were verified through diagnostic plots. Tukey's range test was used for post-hoc comparison.

Results

Piperonylic acid (PA) treatment induces systemic plant resistance against plant-parasitic nematodes, without negative effects on plant growth and development

Foliar PA pre-treatment enhanced resistance to the root-knot nematode *Meloidogyne incognita*, as evidenced by a reduced number of galls 28 dai (-56%, $P < 0.001$), an effect that showed no dose-dependence over the tested concentration range (100 - 1000 μM ; **Figure 1a**). PA also induced resistance against the rice root-knot nematode *M. graminicola* at 14 dai (-40%, $P < 0.001$; **Figure 1b**). As PA is not acutely toxic to *M. incognita* or *M. graminicola* (**Table 1**), reduced susceptibility is likely due to induced resistance (IR) rather than direct toxicity. Our data suggest a conservation of PA-IR between dicots and monocots.

To verify that PA-IR is not triggered by an unknown off-target effect of PA, we tested whether two other previously described C4H inhibitors, 4-Propynyloxybenzoic acid and 3-(4-Pyridyl)-acrylic acid (Schoch *et al.* 2002), also induced resistance against *M. graminicola* in rice (see **Supplementary Figure S1**). Since these two inhibitors induced the same resistant phenotype as PA, despite their very different chemical structures and inhibition mechanisms (Schoch *et al.* 2002), it is highly likely that C4H inhibition is indeed the root cause of PA-IR.

Since IR may have negative effects on plant growth and development, the effect of weekly foliar PA treatment at concentrations ranging from 100 - 1000 μM on tomato growth was investigated. No effect on leaf area, shoot dry mass or root length was seen ($P = 0.97$, $P = 0.71$ and $P = 0.45$, respectively; **Figures 1c-e**). 300 μM was chosen as the standard dose for all following experiments.

The efficacy of PA-IR against root-knot nematodes was validated in a greenhouse naturally infested with *M. incognita* and *M. javanica*. Soil samples taken before the trial contained 14 000 J2s per liter of soil, indicating a severe infestation.

The effect of PA on plant health and yield was evaluated, and its effect on root-knot nematode disease severity was compared to both an untreated control and the commercial nematicide Cedroz. Both PA and Cedroz reduced disease severity, as indicated by plant gall index ($P = 0.042$ and $P = 0.025$ respectively, **Figure 1f**). By the end of the trial, untreated plants showed a mean gall index (\pm SEM) of 8.1 ± 0.4 , versus 6.3 ± 0.3 in PA-treated plants and 4.6 ± 1.1 in Cedroz-treated plants. Neither treatment significantly affected cumulative yield (PA: +13%, $P = 0.77$; Cedroz: +34%, $P = 0.21$ - **Figure 1g**). No phytotoxicity or growth reduction was observed with any treatment.

Piperonylic acid treatment enhances tomato resistance to the foliar pathogens Botrytis cinerea and Pseudomonas syringae.

Foliar PA treatment enhances resistance against two foliar pathogens, *B. cinerea* R16 (**Figure 2a-c**) and *P. syringae* DC3000 (**Figure 2d**). PA treatment increased the percentage of resistant interactions with *B.*

cinerea from 34% in the control to 64% ($P = 0.014$), and inoculation sites also exhibited higher F_v/F_m (and thus higher photosynthetic efficiency) in PA-treated plants (+11%, $P = 0.018$). In an experiment with higher disease pressure, PA pre-treatment still reduced *B. cinerea* disease pressure (3% resistant interactions in mock-treated plants versus 34% in PA-treated plants, $P < 0.001$; **Supplementary Figure S2a**) and again increased F_v/F_m (+20%, $P = 0.003$; **Supplementary Figure S2b**). Reduced *B. cinerea* disease severity was also observed in a greenhouse experiment with strawberry (*Fragaria x ananassa* Duchesne ‘Elsanta’), shown in

Supplementary Figure S3.

PA-pretreatment similarly reduced tomato susceptibility to *P. syringae* DC3000, as the mean number of specks per cm^2 of leaf area in the first and second leaves was reduced by 33% and 50% respectively ($P = 0.038$ and $P < 0.001$). In the third leaf, which was still emerging, there was no significant effect ($P = 0.11$). As PA is not acutely toxic to either *P. syringae* or *B. cinerea* (**Table 1**), the reduced disease severity is likely caused by IR.

PA treatment reduces the population growth of arthropod herbivores on tomato

The reproduction of three arthropods pests of tomato, the mites *T. urticae* and *A. lycopersici* (Vervaeet, De Vis, De Clercq & Van Leeuwen 2021) and the insect *F. occidentalis*, was significantly lower on PA-pretreated tomato plants. As shown in **Figure 2**, *T. urticae* had 54% fewer living offspring ($P < 0.001$) on PA-treated plants, *A. lycopersici* 63% fewer ($P = 0.002$) and *F. occidentalis* 40% fewer ($P < 0.001$). PA similarly induced resistance against *F. occidentalis* in pepper (*Capsicum annum* L. ‘Cayenne Long Slim’), as shown in **Supplementary Figure S4**. As PA is not acutely toxic to these arthropods (**Table 1**), their reduced reproductive rate is likely caused by PA-IR.

PA treatment induces genome-wide transcriptional changes consistent with IR

To gain insights into the molecular mechanisms behind PA-IR, mRNA from roots and shoots of PA-treated tomato plants was sequenced. By sequencing root and shoot samples, both local responses (shoots) and systemic (roots) transcriptional responses were analyzed. Principal component analysis and hierarchical clustering showed that PA treatment led to substantial transcriptome shifts in both tissues (**Figure 3**). When comparing PA-treated and mock-treated plants, 164 genes were differentially expressed (DE) in shoots (133 up, 31 down) and 309 in roots (86 up, 223 down). A full list of transcripts and their expression changes can be found in **Supplementary Table S2**.

Local transcriptional response to PA treatment

Gene ontology (GO) analysis identified 69 enriched GO terms in PA-treated shoots compared to mock-treated shoots, of which 23 were related to immunity (e.g., *systemic acquired resistance* and *regulation of immune response*; **Supplementary Table S3**), 11 to abiotic stress and four to photosynthesis. InterPro domain analysis also identified enrichment of immunity- and photosynthesis-related domains (**Supplementary Table S3**).

Among immunity-related genes, 15 genes annotated as encoding pathogenesis-related (PR) proteins were DE in PA-treated shoots, all of which were upregulated. Some of these have been used as IR markers in tomato, e.g. *PR1a* (Schuhegger *et al.* 2006; Martínez-Medina *et al.* 2017). Other genes involved in IR are also upregulated in shoots after PA treatment, including four *NIM1-INTERACTING2-like* (*NIMIN2-like*) genes and the tomato ortholog of *Arabidopsis thaliana* *SAD4* (*SAR-DEFICIENT 4*). NIMIN2 is an interactor of NPR1 (Nonexpressor of PR genes) and has a role in IR establishment (Zwicker, Mast, Stos, Pfitzner & Pfitzner 2007), and *SAD4* is involved in the biosynthesis of the immunity regulator L-pipecolic acid (Shan & He 2018). The effect of PA on shoot immunity is further reflected by the induction of six genes encoding WRKY transcription factors.

Both *NIMIN2-like* and *PR1a* are SA-inducible, but no genes known to be involved in SA biosynthesis were DE. There were no clear expression changes in genes involved in abscisic acid, auxin or jasmonic acid biosynthesis and signaling, but two *1-aminocyclopropane-1-carboxylate oxidase-like* genes possibly involved in ethylene biosynthesis were upregulated in shoots.

PA also appears to affect shoot reactive oxygen species (ROS) metabolism, as four genes encoding PEROXIDASES and six encoding GLUTATHIONE-S-TRANSFERASES were upregulated.

Although PA is a well-characterized C4H inhibitor (Schalk *et al.*1998; Schoch *et al.* 2002), our data show no change in shoot expression of *C4H*, nor in that of *PAL* or *4CL*, two other early phenylpropanoid pathway (PPP) gene families. However, several downstream PPP-related genes were upregulated: seven genes involved in flavonoid biosynthesis and glycosylation (two putative *FLAVANONE-3-HYDROXYLASES*, one putative *ISOFLAVONE-2'-HYDROXYLASE* and four *UDP-GLYCOSYLTRANSFERASES* acting on flavonoids, including *TOMATO WOUND-INDUCED 1*) and three genes involved in lignification and cell wall reinforcement (*Caffeoyl-CoA-O-methyltransferase 1*, a *cinnamyl alcohol dehydrogenase* and *THT1-3*, an *N-hydroxycinnamoyl-CoA:tyramine N-hydroxycinnamoyl transferase*). Several other genes involved in cell wall development were also upregulated, including a *CELLULOSE SYNTHASE* and two *GLYCINE-RICH CELL WALL PROTEINS*. Together, these results suggest active cell wall remodeling upon PA treatment.

Systemic transcriptional response to PA treatment -

To investigate the effect of foliar PA application on gene expression in systemic (untreated) tissues, mRNA-sequencing was performed on roots of PA-treated tomato plants. GO analysis of DE genes in roots is consistent with an IR phenotype, 20 out of 45 enriched GO terms were related to plant immunity and five to abiotic stress response (**Supplementary Table S3**).

As in shoots, foliar PA treatment strongly induced PR gene expression in roots: 16 genes annotated as possible PR genes were DE, of which 14 were upregulated. Again as in shoots, these PR genes include IR markers such as *PR1a*. ROS metabolism might also be altered in roots upon PA treatment: four *PEROXIDASES*, one *LACCASE* and one *CATALASE* (but no *GLUTATHIONE-S-TRANSFERASES*) were upregulated.

In contrast to PR- and ROS-related genes, WRKY and ERF transcription factors show a divergent expression pattern between root and shoot after PA treatment. While five *WRKY* genes were upregulated in shoots after PA treatment, seven were downregulated in roots and none upregulated. Genes encoding ETHYLENE RESPONSE FACTORS (ERFs), another major class of transcription factors involved in biotic stress response, also show a contrasting expression pattern between root and shoot: in shoots one such gene is upregulated, whereas in roots nine *ERF* genes were downregulated and three upregulated.

The expression of PPP and cell wall remodeling genes upon PA treatment also differs between shoot and root. One *PAL* gene (Solyc09g007900.5) is downregulated in roots after PA treatment, but no other early PPP genes are DE. One *Hydroxycinnamoyl-CoA-quinic transferase* involved in chlorogenic acid biosynthesis and one *SINAPATE GLUCOSYLTRANSFERASE* were upregulated, but – in marked contrast to shoots – no genes related to flavonoid biosynthesis were DE. Several cell wall-related genes were DE in roots of PA-treated plants: two *cellulose synthases* and *THT1-3* were downregulated, whereas *Xyloglucan endotransglucosylase/hydrolase* and two *pectinesterases* were upregulated.

RT-qPCR validation of mRNA sequencing and time course analysis

To validate mRNA-sequencing results and to investigate the temporal dynamics of PA-IR, twelve genes were chosen for RT-qPCR analysis in a time-course experiment. These genes were selected based on differential expression after PA treatment in the mRNA-sequencing dataset, and because they covered most pathways or groups of functionally related genes identified in the mRNA-sequencing data (see **Supplementary Table S1**).

Gene expression was measured at three time points (6, 24 and 72 hours after PA treatment) in root and shoot to study the spatiotemporal evolution of the plant response to PA (**Figure 4**). There was signi-

ficant agreement between mRNA-seq and RT-qPCR data at 24 hours (Spearman's $\rho = 0.57$, $P = 0.003$; **Supplementary Figure S5**), which supports the validity of our mRNA-sequencing results.

For most genes assayed via RT-qPCR, PA-treated shoot samples showed the highest differential expression after 6 and 24 hours. Root samples showed a smaller fold change at 6 hours, followed by greater differences after 24 and 72 hours. This hints at a temporal difference in gene expression changes after PA treatment, with (directly treated) shoots showing a more rapid response than (systemic) roots.

PA treatment induces a localized ROS burst

To investigate whether upregulation of peroxidase genes in PA-treated shoots (see e.g. *POX51* induction in **Figure 4**) is indicative of altered ROS metabolism, histological staining with 3,3-diaminobenzidine (DAB) was executed on tomato leaflets pre-treated with droplets of a PA or mock solution. Sites of PA droplets showed faint staining one hour PA application, intense staining at three and six hours and faint staining after 24 hours (**Figure 5a** and **5c**). The size of the stained area did not exceed that of the PA droplet, which suggests that intense ROS accumulation after PA treatment is a local phenomenon.

To further test the hypothesis that ROS metabolism is affected by PA treatment, guaiacol peroxidase activity was measured in shoots and roots sampled 24 hours after the second foliar PA treatment. PA treatment increased guaiacol peroxidase activity in shoots (+58%, $P < 0.001$; **Figure 5b**), but not in roots ($P = 0.91$), which further suggests that PA treatment locally affects ROS metabolism.

PA treatment induces extensive metabolic reprogramming

Untargeted UPLC-MS/MS profiling of shoots and roots of tomato seedlings 24h after the second PA treatment was used to further investigate the molecular basis of PA-IR.

After pre-processing, 4692 features were retained in shoots, of which 1672 were differentially abundant (DA). 985 features were more abundant in PA-treated than in mock-treated shoots, whereas 687 were less abundant. A substantial number of DA features were unique to either mock (17)- or PA-treated (396) samples. In roots, 2549 features were retained, of which 186 were significantly DA between PA- and mock-treated samples - a much smaller proportion than in shoots. There was a clear bias towards overaccumulation after PA treatment in roots: 177 features were significantly more abundant, while 9 were less abundant. The smaller effect of PA on the root metabolome is reflected by principal component analysis and hierarchical clustering, both of which show complete separation between PA- and mock-treated shoot samples, but only partial separation for root samples (**Figure 6**).

Pathway analysis identified five metabolic pathways enriched upon PA treatment in tomato shoots: *phenylpropanoid biosynthesis* ($P < 0.001$), *stilbenoid and diarylheptanoid biosynthesis* ($P < 0.001$), *flavonoid biosynthesis* ($P = 0.020$), *riboflavin metabolism* ($P < 0.001$) and *thiamine metabolism* ($P = 0.030$). In roots, four pathways were enriched: *phenylpropanoid biosynthesis* ($P < 0.001$), *stilbenoid and diarylheptanoid biosynthesis* ($P < 0.001$), *flavonoid biosynthesis* ($P = 0.040$) and *galactose metabolism* ($P = 0.030$). A full list of pathways is shown in **Supplementary Table S4**.

PA itself was found in both shoot and root samples from PA-treated plants, both as free PA and as a hexose conjugate. This indicates that PA is taken up, conjugated and possibly systemically transported *in planta*. The hexose conjugate was eleven times more abundant than free PA in shoots, and thirteen times more abundant in roots. Both free and conjugated PA were approximately ten times more abundant in shoots than in roots.

A second feature of interest is the defense hormone SA, which was 6.2 times more abundant in PA-treated than in mock-treated shoots ($P < 0.001$). By contrast, SA abundance in roots was unaffected by foliar PA treatment. To confirm the effect of PA treatment on SA seen after untargeted metabolome profiling, and to verify the absence of responses to other major plant hormones suggested by our transcriptome data, we also performed targeted UPLC-MS/MS measurement of SA, JA, abscisic acid and indole-3-acetic

acid. We observed a similar SA accumulation in tomato shoots after PA treatment (4.8-fold increase) in this experiment, and found no major changes in the level of the other measured phytohormones (**Supplementary Table S6**).

Since foliar PA treatment induces SA accumulation in shoots, we investigated whether SA accumulation is necessary for PA-IR by testing the efficacy of PA in tomato plants expressing the *NahG* transgenic construct, which converts SA to catechol (Brading, Hammond-Kosack, Parr & Jones 2000). Plants expressing *NahG* were more susceptible to *M. incognita* (+14%, $P = 0.037$), confirming the role of SA in defense against *M. incognita* (Martínez-Medina *et al.* 2017). However, PA was almost as effective in *NahG* plants (-36%, $P < 0.001$) as in wild type plants (-43%, $P < 0.001$; **Figure 6**), which suggests that PA-IR against *M. incognita* is at least partially SA-independent.

Besides PA and SA, 59 other DA features were annotated with a high degree of confidence by matching against an in-house database using mass and retention time. A further 226 DA features were putatively annotated to a metabolite class by matching their m/z against the METLIN database (Guijas *et al.* 2018). Both features identified against the in-house database and annotated using METLIN were notably enriched in PPP derivatives and flavonoids. PPP derivatives identified via the in-house database include *para*-coumaroyl quinic acid (4-fold increase after PA treatment, $P < 0.001$), syringin (12-fold increase, $P < 0.001$), feruloyl hexose (3-fold reduction, $P < 0.001$), benzoic acid (66-fold increase, $P < 0.001$) and benzoyl hexose (16-fold increase, $P < 0.001$). The PPP precursor phenylalanine was two times more abundant in PA-treated than in mock-treated shoots ($P < 0.001$). Several PPP derivatives were also DA in roots, but generally with smaller fold changes. Examples include *para*-coumaroyl quinic acid (2.3-fold increase, $P < 0.001$), syringin (2.2-fold increase, $P = 0.031$) and benzoyl hexose (12.6-fold increase, $P = 0.002$).

Among DA features, 153 had m/z values whose only METLIN matches were flavonoids or flavonoid glycosides and whose retention times were compatible with these metabolite classes. Of these 153 features, 67 were less and 86 were more abundant in PA-treated than in mock-treated shoots. Remarkably, 50 of the 86 upregulated flavonoids were unique to PA-treated samples; these flavonoids were either absent in mock-treated plants, or present below the limit of detection. No putative flavonoids were unique to mock-treated samples. In root samples, twelve putative flavonoids were DA, all of which were upregulated and six of which were unique to PA-treated samples.

There is a strong overlap between DA features in root and shoot: 156 out of 186 DA features (84%) in roots were also DA in shoots. Putatively annotated features that were more abundant in both PA-treated roots and shoots include two benzoic acid hexosides, a cinnamoyl hexoside, *para*-coumaroyl quinic acid, a hexose conjugate of 5-hydroxyferulic acid, syringin, seven unidentified flavonoid glycosides and three unidentified flavonoids. A full list of DA features, alongside their empirical formulas and putative annotations, is provided in **Supplementary Table S5**.

The altered metabolome induced by PA treatment impairs M. incognita motility

As PA treatment significantly alters the plant metabolome and reduces tomato susceptibility to *M. incognita*, we wondered whether exposure to a methanol extract from PA- and mock-treated plants would differentially affect the motility of *M. incognita* J2s. As **Figure 7** shows, shoot extracts from PA-treated plants are more nematostatic than shoot extracts from mock-treated plants after 4 and 24 hours of exposure (4 h: $P < 0.001$; 24 h: $P < 0.001$), while root extracts from PA-treated plants are more nematostatic only at 24 hours (4 h: $P = 0.098$; 24 h: $P < 0.001$).

PA pre-treatment primes the accumulation of phenylpropanoid pathway products in nematode-infected roots

To further investigate the effect of PA treatment on the PPP, tomato seedlings were mock- or PA-treated and then either mock-inoculated or inoculated with *M. incognita* 24 hours later. Free and cell-wall bound phenolic substances as well as lignin were quantified in leaves, stems and roots seven days. *M. incognita* infection in PA-treated plants led to a significant increase in the abundance of free phenolic compounds (+25%, $P = 0.013$), cell wall-bound phenolic compounds (+20%, $P = 0.008$) and lignin (+21%, $P = 0.002$) in roots, but

not in (uninfected) stems or leaves (**Figure 8**). Neither PA treatment nor *M. incognita* infection alone affected these parameters.

Together with our metabolome data, these results indicate that PA initially reprograms PPP and flavonoid metabolism without significantly increasing the total abundance of these compounds, while also priming plants for local phenolic compound accumulation upon pathogen attack.

Discussion

Resistance inducers have considerable potential in integrated pest management, but remain rarely used due to concerns including phytotoxicity and limited efficacy (Walters & Fountaine 2009). Our work identifies piperonylic acid (PA) as an effective, broad-spectrum and non-phytotoxic novel resistance inducer. PA treatment significantly reduces the susceptibility of several crop plants to a panel of pests and pathogens that includes organisms with different lifestyles (necrotrophs, (hemi)biotrophs and herbivores), degrees of specialization (generalists and specialists), and host tissues (roots and shoots).

PA is a well-known inhibitor of C4H, the second enzyme of the phenylpropanoid pathway (PPP) (Schalk *et al.* 1998). Prolonged inhibition of this pathway by growing plants on medium containing PA is detrimental to plant growth and development (Naseer *et al.* 2012; Van de Wouwer *et al.* 2016), whereas we show that pulsed PA application has no such effect. The absence of growth defects upon pulse treatment with PA is likely explained by rapid inactivation of PA through conjugation, which we have observed here in tomato and which had previously been reported in *A. thaliana* (Steenackers *et al.* 2016).

Foliar PA treatment does not affect growth, but does trigger several IR hallmarks. PA-treated plants experience a transient, local ROS burst which begins within one hour and peaks several hours later, a response consistent with our understanding of ROS as an early messenger in plant immunity (Nanda, Andrio, Marino, Pauly & Dunand 2010; Barna, Fodor, Harrach, Pogány & Király 2012; Segal & Wilson 2018). Further evidence for altered ROS metabolism after PA treatment is provided by induction of peroxidase-encoding genes and higher shoot guaiacol peroxidase activity, the latter of which has also been reported after exposure to the IR inducer COS-OGA (van Aubel *et al.* 2016). In addition, PA treatment also induces the expression of several IR-associated genes, including *PR1a* (Schuhegger *et al.* 2006; Martínez-Medina *et al.* 2017), *NIMIN2-like* (Zwicker *et al.* 2007) and *SAD4* (Shan & He 2018).

The accumulation of (often glycosylated) PPP derivatives is a hallmark of IR, which has been observed with diverse IR stimuli in several plant species (Mhlongo, Steenkamp, Piater, Madala & Dubery 2016; Gamir *et al.* 2020; Ameye *et al.* 2020; Huang *et al.* 2021). While it is known that PPP perturbation is a *consequence* of IR induction, our research suggests that PPP perturbation, in this case by transient inhibition of C4H, can also be a *cause* of IR. Based on our results, we propose a model of PA-IR outlined in which transient C4H inhibition by PA leads to an initial PPP perturbation, which results in the accumulation of (unidentified) PPP-derived immune-signaling metabolites and, eventually, IR establishment. The PA-IR state includes primed lignification and phenolic compound accumulation, induction of PR genes and accumulation of (likely PPP-derived) nematostatic metabolites.

In this model, PPP-derived metabolites contribute to PA-IR in multiple ways. First, PPP derivatives are involved in PA-IR signaling, a role consistent with the known role of flavonoids and other PPP-derivatives in plant immune regulation (Mandal, Chakraborty & Dey 2010; Saijo & Loo 2020). Second, PPP derivatives contribute to the PA-IR phenotype through their roles as phytoanticipins/phytoalexins (Yadav *et al.* 2020; Desmedt *et al.* 2020) and building blocks for cell wall reinforcement (Vogt 2010). Finally, their potent antioxidant activity (Rice-Evans, Miller & Paganga 1997; Agati, Azzarello, Pollastri & Tattini 2012) might help the plant cope with the oxidative stress involved in pathogen attack (Barna *et al.* 2012; Lehmann, Serrano, L'Haridon, Tjamos & Metraux 2015; Segal & Wilson 2018). With regards to the role of PPP derivatives as phytoalexins and phytoanticipins, it is noteworthy that we found that PA-IR induces accumulation of metabolites with a nematostatic effect on *M. incognita*. A similar accumulation of nematostatic compounds upon IR induction has been reported in oat (*Avena sativa*) (Soriano, Asenstorfer, Schmidt & Riley 2004). In addition to direct induction of defense metabolites upon PA treatment, we also found evidence that PA

primes local lignification and phenolic compound accumulation in roots infected by *M. incognita*. Local lignification upon pathogen exposure has previously been implicated in both induced and genetic resistance against various pathogens (Yadav *et al.* 2020), including *P. syringae* (Lee *et al.* 2019) and *M. incognita* (Veronico *et al.* 2018).

When considering potential metabolites involved in initial IR establishment upon PPP perturbation, it is tempting to look at the defense hormone SA. SA accumulates in PA-treated shoots, and SA accumulation is a known IR marker in dicots (Pieterse *et al.* 2014). However, we found that PA-IR was largely preserved in tomato plants impaired in SA accumulation. SA-independence has also been shown for IR stimuli including COS-OGA and beta-aminobutyric acid in various pathosystems (Cohen, Vaknin & Mauch-Mani 2016; Singh *et al.* 2019).

Metabolites involved in PA-IR signaling might instead be found amongst (glycosylated) flavonoids and phenylpropanoids, as several such metabolites show a very large increase in abundance after PA treatment. Several genes encoding glycosyltransferases acting on flavonoids and phenylpropanoids were induced by PA treatment, including *TOMATO WOUND-INDUCED 1 (Twi1)*. *Twi1* encodes a promiscuous glycosyltransferase acting on various benzoic acids, flavonoids and coumarins (Campos *et al.* 2019). *Twi1* silencing perturbs flavonoid metabolism and increases susceptibility to tomato spotted wilt virus (Campos *et al.* 2019). Although *Twi1* is SA-inducible, the continued ability of elicitors to induce *Twi1* in tomato plants expressing the *NahG* construct suggests the existence of SA-independent *Twi1* regulation (O'Donnell *et al.* 1998). Interestingly, *Twi1* is already upregulated 6 hours after PA treatment in shoots and roots and remains upregulated by 72 hours in both tissues, indicating that *Twi1* induction is an early, systemic and relatively long-lived response to PA treatment. In support of a regulatory role for phenylpropanoid and flavonoid glycosylation in plant immunity, it was recently shown that the *A. thaliana* glycosyltransferase *UGT73C7*, which glycosylates phenylpropanoids including *para*-coumaric acid and ferulic acid, plays a major role in *A. thaliana* immunity against *P. syringae* and that its overexpression leads to constitutive PR gene induction and SA accumulation (Huang *et al.* 2021).

A key feature of IR is that it is a systemic as well as a local phenomenon (Vlot *et al.* 2020). A systems biology view of PA-IR reveals considerable differences between (systemic) roots and (directly treated) shoots. Whereas the root metabolome is much less affected by PA treatment than the shoot metabolome, the transcriptional response (as measured by the number of differentially expressed genes) to PA treatment is comparable in magnitude. This suggests that PA-IR involves systemic transcriptional changes, while direct accumulation of (defense-related) metabolites is mostly confined to local tissues. By contrast, metabolome analysis of tomato plants foliarly treated with oligogalacturonides found greater metabolic changes in distal root tissues than in directly treated leaves (Gamir *et al.* 2020).

Our data are compatible with at least two - non-exclusive - explanations for the systemic spread of PA-IR. The first is that metabolites with IR signaling functions, most likely PPP-derived, are transported from treated to distal tissues. In tentative support of this hypothesis, it can be noted that the metabolites which accumulate in systemic root tissues during PA-IR form a small subset of those accumulating in directly treated shoot tissues. A second possibility is that the small quantities of PA found in roots after foliar PA treatment are sufficient for establishing PA-IR in roots. Grafting experiments combined with further metabolomic analysis might elucidate the role of metabolite transport in PA-IR.

Although the precise mechanisms behind PA-IR induction and spread remain to be fully elucidated, our research shows that PA-IR is broad-spectrum and that the PA-IR phenotype appears to be conserved amongst flowering plants. While further multi-season and multi-location field trials as well as ecotoxicological assessments will be required before PA can be used in agriculture, our results – which include data from a field trial in naturally nematode-infested soil - indicate the potential of PA as a sustainable crop protection product.

Acknowledgments

The authors thank Prof. Dr. Els Van Damme (Ghent University) for providing *P. syringae* DC3000, Prof. Dr. Eduardo de la Pena (Ghent University) and Lidia Blanco Sánchez (Institute for Mediterranean and

Subtropical Horticulture) for providing tomato *NahG* and corresponding Moneymaker wild type seeds, Lien De Smet (Ghent University) for technical support with mRNA extraction and RT-qPCR, and Emanuele Medico (Eastman) for organizing and overseeing the field trial. This work was supported a Baekeland grant (HBC.2017.0574) awarded to WD, which was jointly funded by the Flemish government's Agency for Innovation and Entrepreneurship (VLAIO) and Taminco, an Eastman subsidiary. Two patent applications describing the use of C4H inhibitors as crop protection products have been published (WO2019122107A1 and WO2020127216A1). WD, BVH and TK are the inventors of patent WO2019122107A1 and WD, TVL, BVH and TK are the inventors of patent WO2020127216A1. The other authors have no potential conflicts of interest to disclose.

References

- Van Acker R., Vanholme R., Storme V., Mortimer J.C., Dupree P. & Boerjan W. (2013) Lignin biosynthesis perturbations affect secondary cell wall composition and saccharification yield in *Arabidopsis thaliana*. *Biotechnology for Biofuels* **6** , 46.
- Agati G., Azzarello E., Pollastri S. & Tattini M. (2012) Flavonoids as antioxidants in plants: Location and functional significance. *Plant Science* **196** , 67–76.
- Ahuja I., Kissen R. & Bones A.M. (2012) Phytoalexins in defense against pathogens. *Trends in Plant Science* **17** , 73–90.
- Ainsworth E.A. & Gillespie K.M. (2007) Estimation of total phenolic content and other oxidation substrates in plant tissues using Folin–Ciocalteu reagent. *Nature Protocols* **2** , 875–877.
- Ameye M., Van Meulebroek L., Meuninck B., Vanhaecke L., Smagghe G., Haesaert G. & Audenaert K. (2020) Metabolomics Reveal Induction of ROS Production and Glycosylation Events in Wheat Upon Exposure to the Green Leaf Volatile Z-3-Hexenyl Acetate. *Frontiers in Plant Science* **11** , 1854.
- Andrews S. (2010) FastQC: A Quality Control tool for High Throughput Sequence Data.
- van Aubel G., Buonatesta R. & Van Cutsem P. (2014) COS-OGA: A novel oligosaccharidic elicitor that protects grapes and cucumbers against powdery mildew. *Crop Protection* **65** , 129–137.
- van Aubel G., Cambier P., Dieu M. & Van Cutsem P. (2016) Plant immunity induced by COS-OGA elicitor is a cumulative process that involves salicylic acid. *Plant Science* **247** , 60–70.
- Audenaert K., De Meyer G.B. & Höfte M.M. (2002) Abscisic acid determines basal susceptibility of tomato to *Botrytis cinerea* and suppresses salicylic acid-dependent signaling mechanisms. *Plant Physiology* **128** , 491–501.
- Balmer A., Pastor V., Gamir J., Flors V. & Mauch-Mani B. (2015) The ‘prime-ome’: towards a holistic approach to priming. *Trends in Plant Science* **20** , 443–452.
- Barna B., Fodor J., Harrach B.D., Pogány M. & Király Z. (2012) The Janus face of reactive oxygen species in resistance and susceptibility of plants to necrotrophic and biotrophic pathogens. *Plant Physiology and Biochemistry* **59** , 37–43.
- Barnes W. & Anderson C. (2017) Acetyl Bromide Soluble Lignin (ABSL) Assay for Total Lignin Quantification from Plant Biomass. *Bio-protocol* **7** .
- Van Bel M., Diels T., Vancaester E., Kreft L., Botzki A., Van De Peer Y., ... Vandepoele K. (2018) PLAZA 4.0: An integrative resource for functional, evolutionary and comparative plant genomics. *Nucleic Acids Research* **46** , D1190–D1196.
- Blancard D. (2013) *Tomato Diseases: Identification, Biology and Control: A Colour Handbook* , 2nd ed. CRC Press, Boca Raton.

- Bolger A.M., Lohse M. & Usadel B. (2014) Trimmomatic: a flexible trimmer for Illumina sequence data. *Bioinformatics (Oxford, England)* **30** , 2114–20.
- Bolstad B.M., Irizarry R.A., Åstrand M. & Speed T.P. (2003) A comparison of normalization methods for high density oligonucleotide array data based on variance and bias. *Bioinformatics***19** , 185–193.
- Brading P.A., Hammond-Kosack K.E., Parr A. & Jones J.D. (2000) Salicylic acid is not required for Cf-2- and Cf-9-dependent resistance of tomato to *Cladosporium fulvum*. *The Plant journal : for cell and molecular biology* **23** , 305–18.
- La Camera S., Gouzerh G., Dhondt S., Hoffmann L., Fritig B., Legrand M. & Heitz T. (2004) Metabolic reprogramming in plant innate immunity: the contributions of phenylpropanoid and oxylipin pathways. *Immunological Reviews* **198** , 267–284.
- Campos L., Lopez-Gresa M.P., Fuertes D., Belles J.M., Rodrigo I. & Lison P. (2019) Tomato glycosyltransferase Twil plays a role in flavonoid glycosylation and defence against virus. *BMC Plant Biology* **19** , 1–17.
- Cheng Y., Bian W., Pang X., Yu J., Ahammed G.J., Zhou G., ... Wan H. (2017) Genome-wide identification and evaluation of reference genes for quantitative RT-PCR analysis during tomato fruit development. *Frontiers in Plant Science* **8** .
- Chezem W.R., Memon A., Li F.S., Weng J.K. & Clay N.K. (2017) SG2-type R2R3-MYB transcription factor MYB15 controls defense-induced lignification and basal immunity in arabidopsis. *Plant Cell***29** , 1907–1926.
- Chong J., Wishart D.S. & Xia J. (2019) Using MetaboAnalyst 4.0 for comprehensive and integrative metabolomics data analysis. *Current Protocols in Bioinformatics* **68** .
- Cohen Y., Vaknin M. & Mauch-Mani B. (2016) BABA-induced resistance: milestones along a 55-year journey. *Phytoparasitica* **44** , 513–538.
- Conrath U., Beckers G.J.M., Flors V., Garcia-Agustin P., Jakab G., Mauch F., ... Mauch-Mani B. (2006) Priming: Getting Ready for Battle. *Molecular Plant-Microbe Interactions* **19** , 1062–1071.
- Conrath U., Beckers G.J.M., Langenbach C.J.G. & Jaskiewicz M.R. (2015) Priming for Enhanced Defense. *Annual Review of Phytopathology***53** , 97–119.
- Daudi A. & O'Brien J. (2012) Detection of Hydrogen Peroxide by DAB Staining in Arabidopsis Leaves. *Bio-protocol* **2** .
- Dempsey D.A., Vlot A.C., Wildermuth M.C. & Klessig D.F. (2011) Salicylic Acid Biosynthesis and Metabolism. *The Arabidopsis Book***9** .
- Desmedt W., Mangelinckx S., Kyndt T. & Vanholme B. (2020) A Phytochemical Perspective on Plant Defense Against Nematodes. *Frontiers in Plant Science* **11** , 1765.
- Dixon R.A., Achnine L., Kota P., Liu C.J., Reddy M.S.S. & Wang L. (2002) The phenylpropanoid pathway and plant defence - A genomics perspective. *Molecular Plant Pathology* **3** , 371–390.
- Dobin A. & Gingeras T.R. (2015) Mapping RNA-seq Reads with STAR. *Current protocols in bioinformatics* **51** , 11.14.1-19.
- Durbin B.P., Hardin J.S., Hawkins D.M. & Rocke D.M. (2002) A variance-stabilizing transformation for gene-expression microarray data. In *Bioinformatics* . Oxford University Press.
- Faretra F. & Pollastro S. (1991) Genetic basis of resistance to benzimidazole and dicarboximide fungicides in *Botryotinia fuckeliana* (*Botrytis cinerea*). *Mycological Research* **95** , 943–951.
- Gamir J., Minchev Z., Berrio E., Garcia J.M., De Lorenzo G. & Pozo M.J. (2020) Roots drive oligogalacturonide-induced systemic immunity in tomato. *Plant, Cell & Environment* .

- Ghaemi R., Pourjam E., Safaie N., Verstraeten B., Mahmoudi S.B., Mehrabi R., ... Kyndt T. (2020) Molecular insights into the compatible and incompatible interactions between sugar beet and the beet cyst nematode. *BMC Plant Biology* **20** , 483.
- Gould W.A. (1992) *Tomato Production, Processing and Technology* , 3rd ed. CTI Publications, Baltimore.
- Guijas C., Montenegro-Burke J.R., Domingo-Almenara X., Palermo A., Warth B., Hermann G., ... Siuzdak G. (2018) METLIN: A Technology Platform for Identifying Knowns and Unknowns. *Analytical Chemistry* **90** , 3156–3164.
- Haeck A., Van Langenhove H., Harinck L., Kyndt T., Gheysen G., Hofte M. & Demeestere K. (2018) Trace analysis of multi-class phytohormones in *Oryza sativa* using different scan modes in high-resolution Orbitrap mass spectrometry: method validation, concentration levels, and screening in multiple accessions. *Analytical and Bioanalytical Chemistry* **410** , 4527–4539.
- Hallmann J. & Viaene N. (2013) PM 7/119 (1) Nematode extraction. *EPPO Bulletin* **43** , 471–495.
- Hosmani P.S., Flores-Gonzalez M., van de Geest H., Maumus F., Bakker L. V., Schijlen E., ... Saha S. (2019) An improved de novo assembly and annotation of the tomato reference genome using single-molecule sequencing, Hi-C proximity ligation and optical maps. *bioRxiv* , 767764.
- Huang X., Wang Y., Lin J., Chen L., Li Y., Liu Q., ... Hou B. (2021) A novel pathogen-responsive glycosyltransferase UGT73C7 mediates the redirection of phenylpropanoid metabolism and promotes *SNC1*-dependent Arabidopsis immunity. *The Plant Journal* , tpj.15280.
- De Kesel J., Conrath U., Flors V., Luna E., Mageroy M.H., Mauch-Mani B., ... Kyndt T. (2021) The Induced Resistance Lexicon: Do's and Don'ts. *Trends in Plant Science* .
- De Kesel J., Gomez-Rodriguez R., Bonneure E., Mangelinckx S. & Kyndt T. (2020) The Use of PTI-Marker Genes to Identify Novel Compounds that Establish Induced Resistance in Rice. *International Journal of Molecular Sciences* **21** , 317.
- Lawrence M., Huber W., Pages H., Aboyoun P., Carlson M., Gentleman R., ... Carey V.J. (2013) Software for Computing and Annotating Genomic Ranges. *PLoS Computational Biology* **9** , e1003118.
- Lee M., Jeon H.S., Kim S.H., Chung J.H., Roppolo D., Lee H., ... Park O.K. (2019) Lignin-based barrier restricts pathogens to the infection site and confers resistance in plants. *The EMBO Journal* **38** .
- Lehmann S., Serrano M., L'Haridon F., Tjamos S.E. & Metraux J.P. (2015) Reactive oxygen species and plant resistance to fungal pathogens. *Phytochemistry* **112** , 54–62.
- Li S., Park Y., Duraisingham S., Strobel F.H., Khan N., Soltow Q.A., ... Pulendran B. (2013) Predicting Network Activity from High Throughput Metabolomics. *PLoS Computational Biology* **9** , 1003123.
- van Loon L.C., Rep M. & Pieterse C.M.J. (2006) Significance of Inducible Defense-related Proteins in Infected Plants. *Annual Review of Phytopathology* **44** , 135–162.
- Love M.I., Huber W. & Anders S. (2014) Moderated estimation of fold change and dispersion for RNA-seq data with DESeq2. *Genome Biology* **15** , 550.
- Luna E., Pastor V., Robert J., Flors V., Mauch-Mani B. & Ton J. (2011) Callose Deposition: A Multifaceted Plant Defense Response. / *183 MPMI* **24** , 183–193.
- MacAdam J.W., Nelson C.J. & Sharp R.E. (1992) Peroxidase activity in the leaf elongation zone of tall fescue: I. Spatial distribution of ionically bound peroxidase activity in genotypes differing in length of the elongation zone. *Plant Physiology* **99** , 872–878.
- Malinovsky F.G., Fangel J.U. & Willats W.G.T. (2014) The role of the cell wall in plant immunity. *Frontiers in Plant Science* **5** , 178.

- Mandal S.M., Chakraborty D. & Dey S. (2010) Phenolic acids act as signaling molecules in plant-microbe symbioses. *Plant Signaling & Behavior* **5** , 359–368.
- Martinez-Medina A., Fernandez I., Lok G.B., Pozo M.J., Pieterse C.M.J. & Van Wees S.C.M. (2017) Shifting from priming of salicylic acid- to jasmonic acid-regulated defences by Trichoderma protects tomato against the root knot nematode *Meloidogyne incognita*. *New Phytologist* **213** , 1363–1377.
- Martinez-Medina A., Flors V., Heil M., Mauch-Mani B., Pieterse C.M.J., Pozo M.J.M.J., ... Conrath U. (2016) Recognizing Plant Defense Priming. *Trends in Plant Science* **21** , 818–822.
- Mathesius U. (2018) Flavonoid functions in plants and their interactions with other organisms. *Plants* **7** .
- Mauch-Mani B., Baccelli I., Luna E. & Flors V. (2017) Defense priming: An adaptive part of induced resistance. *Annual Review of Plant Biology* **68** , 485–512.
- De Meester B., De Vries L., Ozparpucu M., Gierlinger N., Corneillie S., Pallidis A., ... Boerjana W. (2018) Vessel-specific reintroduction of CINNAMOYL-COA REDUCTASE1 (CCR1) in Dwarfed ccr1 mutants restores vessel and Xylary fiber integrity and increases biomass. *Plant Physiology* **176** , 611–633.
- Meng L., Mestdagh H., Ameye M., Audenaert K., Hofte M. & Van Labeke M.C. (2020) Phenotypic Variation of Botrytis cinerea Isolates Is Influenced by Spectral Light Quality. *Frontiers in Plant Science* **11** .
- Mhlongo M.I., Steenkamp P.A., Piater L.A., Madala N.E. & Dubery I.A. (2016) Profiling of Altered Metabolomic States in Nicotiana tabacum Cells Induced by Priming Agents. *Frontiers in Plant Science* **7** .
- Miedes E., Vanholme R., Boerjan W. & Molina A. (2014) The role of the secondary cell wall in plant resistance to pathogens. *Frontiers in plant science* **5** , 358.
- Nahar K., Kyndt T., De Vleeschauwer D., Hofte M. & Gheysen G. (2011) The Jasmonate Pathway Is a Key Player in Systemically Induced Defense against Root Knot Nematodes in Rice. *Plant physiology* **157** , 305–316.
- Nanda A.K., Andrio E., Marino D., Pauly N. & Dunand C. (2010) Reactive Oxygen Species during Plant-microorganism Early Interactions. *Journal of Integrative Plant Biology* **52** , 195–204.
- Naseer S., Lee Y., Lapierre C., Franke R., Nawrath C. & Geldner N. (2012) Casparian strip diffusion barrier in Arabidopsis is made of a lignin polymer without suberin. *Proceedings of the National Academy of Sciences of the United States of America* **109** , 10101–10106.
- O'Donnell P.J., Truesdale M.R., Calvert C.M., Dorans A., Roberts M.R. & Bowles D.J. (1998) A novel tomato gene that rapidly responds to wound- and pathogen-related signals. *Plant Journal* **14** , 137–142.
- Obermeier C., Hossain M.A., Snowdon R., Knufer J., von Tiedemann A. & Friedt W. (2013) Genetic analysis of phenylpropanoid metabolites associated with resistance against *Verticillium longisporum* in Brassica napus. *Molecular Breeding* **31** , 347–361.
- Perazzolli M., Roatti B., Bozza E. & Pertot I. (2011) Trichoderma harzianum T39 induces resistance against downy mildew by priming for defense without costs for grapevine. *Biological Control* **58** , 74–82.
- Pieterse C.M.J., Zamioudis C., Berendsen R.L., Weller D.M., Van Wees S.C.M. & Bakker P.A.H.M. (2014) Induced systemic resistance by beneficial microbes. *Annual Review of Phytopathology* **52** , 347–375.
- Ranjan A., Westrick N.M., Jain S., Piotrowski J.S., Ranjan M., Kessens R., ... Kabbage M. (2019) Resistance against *Sclerotinia sclerotiorum* in soybean involves a reprogramming of the phenylpropanoid pathway and up-regulation of antifungal activity targeting ergosterol biosynthesis. *Plant Biotechnology Journal* **17** , 1567–1581.
- Rice-Evans C.A., Miller N.J. & Paganga G. (1997) Antioxidant properties of phenolic compounds. *Trends in Plant Science* **2** , 152–159.

- Romero A.M., Kousik C.S. & Ritchie D.F. (2001) Resistance to Bacterial Spot in Bell Pepper Induced by Acibenzolar- *S* -Methyl. *Plant Disease* **85** , 189–194.
- Ruijter J.M., Ramakers C., Hoogaars W.M.H., Karlen Y., Bakker O., van den hoff M.J.B. & Moorman A.F.M. (2009) Amplification efficiency: Linking baseline and bias in the analysis of quantitative PCR data. *Nucleic Acids Research* **37** , e45–e45.
- Saijo Y. & Loo E.P. (2020) Plant immunity in signal integration between biotic and abiotic stress responses. *New Phytologist* **225** , 87–104.
- Schalk M., Cabello-Hurtado F., Pierrel M.-A.A., Atanossova R., Saindrenan P. & Werck-Reichhart D. (1998) Piperonylic acid, a selective, mechanism-based inactivator of the trans-cinnamate 4-hydroxylase: A new tool to control the flux of metabolites in the phenylpropanoid pathway. *Plant physiology* **118** , 209–18.
- Schoch G.A., Nikov G.N., Alworth W.L. & Werck-Reichhart D. (2002) Chemical inactivation of the cinnamate 4-hydroxylase allows for the accumulation of salicylic acid in elicited cells. *Plant physiology* **130** , 1022–31.
- Schuhegger R., Ihring A., Gantner S., Bahnweg G., Knappe C., Vogg G., ... Langebartels C. (2006) Induction of systemic resistance in tomato by N-acyl-L-homoserine lactone-producing rhizosphere bacteria. *Plant, Cell and Environment* **29** , 909–918.
- Segal L.M. & Wilson R.A. (2018) Reactive oxygen species metabolism and plant-fungal interactions. *Fungal Genetics and Biology* **110** , 1–9.
- Shan L. & He P. (2018) Pipped at the post: pipercolic acid derivative identified as SAR regulator. *Cell* **173** , 286–287.
- Singh R.R., Chinnasri B., De Smet L., Haeck A., Demeestere K., Van Cutsem P., ... Kyndt T. (2019) Systemic defense activation by COS-OGA in rice against root-knot nematodes depends on stimulation of the phenylpropanoid pathway. *Plant Physiology and Biochemistry* **142** , 202–210.
- Soriano I.R., Asenstorfer R.E., Schmidt O. & Riley I.T. (2004) Inducible flavone in oats (*Avena sativa*) is a novel defense against plant-parasitic nematodes. *Phytopathology* **94** , 1207.
- Steenackers W.J., Cesarino I., Klima P., Quareshy M., Vanholme R., Corneillie S., ... Vanholme B. (2016) The allelochemical MDCA inhibits lignification and affects auxin homeostasis. *Plant physiology* .
- Veronico P., Paciolla C., Pomar F., De Leonardis S., Garcia-Ulloa A. & Melillo M.T. (2018) Changes in lignin biosynthesis and monomer composition in response to benzothiadiazole and root-knot nematode *Meloidogyne incognita* infection in tomato. *Journal of Plant Physiology* **230** , 40–50.
- Vervaeet L., De Vis R., De Clercq P. & Van Leeuwen T. (2021) Is the emerging mite pest *Aculops lycopersici* controllable? Global and genome-based insights in its biology and management. *Pest Management Science* , ps.6265.
- Vlot A.C., Sales J.H., Lenk M., Bauer K., Brambilla A., Sommer A., ... Nayem S. (2020) Systemic propagation of immunity in plants. *New Phytologist* , nph.16953.
- Vogt T. (2010) Phenylpropanoid biosynthesis. *Molecular Plant* **3** , 2–20.
- Walters D.R. & Fountaine J.M. (2009) Practical application of induced resistance to plant diseases: An appraisal of effectiveness under field conditions. *Journal of Agricultural Science* **147** , 523–535.
- Wang R., Wang G.L. & Ning Y. (2019) PALs: Emerging Key Players in Broad-Spectrum Disease Resistance. *Trends in Plant Science* **24** , 785–787.
- Van de Wouwer D., Vanholme R., Decou R., Goeminne G., Audenaert D., Nguyen L., ... Boerjan W. (2016) Chemical Genetics Uncovers Novel Inhibitors of Lignification, Including p-Iodobenzoic Acid Targeting CINNAMATE-4-HYDROXYLASE. *Plant physiology* **172** , 198–220.

Wybouw N., Zhurov V., Martel C., Bruinsma K.A., Hendrickx F., Grbic V. & Van Leeuwen T. (2015) Adaptation of a polyphagous herbivore to a novel host plant extensively shapes the transcriptome of herbivore and host. *Molecular Ecology* **24** , 4647–4663.

Xue F.C., Chandra R., Berleth T. & Beatson R.P. (2008) Rapid, microscale, acetyl bromide-based method for high-throughput determination of lignin content in *Arabidopsis thaliana*. *Journal of Agricultural and Food Chemistry* **56** , 6825–6834.

Xue W., Snoeck S., Njiru C., Inak E., Dermauw W. & Van Leeuwen T. (2020) Geographical distribution and molecular insights into abamectin and milbemectin cross-resistance in European field populations of *Tetranychus urticae* . *Pest Management Science* **76** , 2569–2581.

Yadav V., Wang Z., Wei C., Amo A., Ahmed B., Yang X. & Zhang X. (2020) Phenylpropanoid pathway engineering: An emerging approach towards plant defense. *Pathogens* **9** , 312.

Yoshioka K., Nakashita H., Klessig D.F. & Yamaguchi I. (2001) Probenazole induces systemic acquired resistance in *Arabidopsis* with a novel type of action. *The Plant journal : for cell and molecular biology* **25** , 149–57.

Zeck W.M. (1971) Rating scheme for field evaluation of root-knot nematode infestations. *Pflanzenschutz Nachrichten Bayer* **24** , 141–144.

Zwicker S., Mast S., Stos V., Pfitzner A.J.P. & Pfitzner U.M. (2007) Tobacco NIMIN2 proteins control PR gene induction through transient repression early in systemic acquired resistance. *Molecular Plant Pathology* **8** , 385–400.

Tables

Table 1: Evaluation of acute in vitro toxicity of piperonylic acid to the pests and pathogens used in this study. Reported values are means \pm SEM. Exposure duration for *A. lycopersici* and *T. urticae* is not given, because these were sprayed with PA instead of being continuously exposed. P-values were calculated using Fisher’s exact test for *M. incognita*, *M. graminicola*, *A. lycopersici*, *T. urticae* and *F. occidentalis* , and using a heteroskedastic T-test for *P. syringae* and *B. cinerea* .

Organism

Variable

Exposure (hours)

PA

(300 μ M)

Control

P-value

N

Meloidogyne incognita

Motile J2s (%)

48

96 \pm 1

97 \pm 1

0.78

6 (6 x 50 J2s)

Meloidogyne graminicola

Motile J2s (%)

48

94 ± 1

94 ± 1

0.46

6 (6 x 50 J2s)

Pseudomonas syringae

OD₆₀₀

24

0.76 ± 0.01

0.74 ± 0.04

0.68

6

Botrytis cinerea

Colony area (cm²)

120

21.1 ± 2.4

20.3 ± 1.4

0.78

6

Aculops lycopersici

Living adults (%)

NA

60 ± 4

57 ± 6

0.77

6 (6 x 25 adults)

Tetranychus urticae

Living adults (%)

NA

96 ± 3

99 ± 2

0.21

6 (6 x 25 adults)

Frankliniella occidentalis

Living larvae (%)

NA

97 ± 1

96 ± 2

1.00

6 (6 x 25 larvae)

Figure legends

Figure 1: The effects of PA treatment on tomato growth and susceptibility to root-knot nematodes. **(a)** Number of galls in the roots of tomato plants 28 days after inoculation with 250 *M. incognita* J2s. **(b)** Number of galls in the roots of rice plants 14 days after inoculation with 250 *M. graminicola* J2s. **(c-e)** Effect of weekly PA treatment on the dry shoot mass (c), leaf area (b) and root system length (c) of tomato seedlings. Treatments with different letters differ significantly ($P < 0.05$). $N = 8$. **(f-g)** Efficacy of PA (applied thrice as a 300 μM foliar spray) at controlling root-knot nematodes in tomato plants grown in soil naturally infested with a mixed population of *M. incognita* and *M. javanica*. Cedroz, a commercial nematicide, was used as reference treatment. PA was applied three times, Cedroz was applied six times according to the manufacturer's instructions. Error bars indicate the standard error of the mean. **(f)** Disease severity (as indicated Zeck's galling index) over the course of the trial. $N = 4$ plots per treatment (from each of which four plants were uprooted and evaluated at the first three time points and ten at the final time point). **(g)** Cumulative yield (in kg tomatoes per plot). $N = 4$ plots per treatment.

Figure 2: Efficacy of PA against foliar pests and diseases of tomato: *Botrytis cinerea*R16, *Pseudomonas syringae* DC3000, *Tetranychus urticae*, *Aculops lycopersici* and *Frankliniella occidentalis*. **(a)** Percentage of *B. cinerea* inoculation sites that led to successful colonization four days after inoculation ($N = 32$ inoculation sites on 8 leaves). **(b)** F_v/F_m (photosynthesis quantum yield) in *B. cinerea* infection sites. **(c)** chlorophyll images of *B. cinerea* inoculation sites in tomato leaves pre-treated with 300 μM piperonylic acid (PA) or a corresponding mock treatment (Control); black coloration indicates *B. cinerea*-induced necrosis. **(d)** Number of *P. syringae* DC3000 specks per cm^2 of leaf area five days after dip inoculation ($N = 12$). **(e)** Number of *T. urticae* offspring present on tomato plants ten days after inoculation with 10 adult females ($N = 8$). **(f)** Number of *A. lycopersici* offspring present on tomato plants ten days after inoculation with 30 mixed-sex mites ($N = 6$). **(g)** Number of *F. occidentalis* offspring present on tomato plants five days after ten adult females were given 24 hours to deposit eggs ($N = 15$).

Figure 3: **(a)** Principal component analysis scatterplot of samples from tomato roots and shoots harvested 24 hours after the second PA or mock treatment (CON), based on mRNA-sequencing based analysis of gene expression. Shaded ellipses represent 95% confidence ellipses. **(b)** Heatmap (showing normalized, centered and scaled expression values) and hierarchical clustering of samples and transcripts from tomato roots and shoots harvested after PA or mock treatment (CON), based on the same dataset as (a).

Figure 4: Gene expression in shoots **(a)** and roots **(b)** of tomato seedlings harvested 6, 24 and 72 hours after the second foliar treatment with 300 μM PA relative to mock-treated control plants. Relative expression values are \log_2 -transformed; error bars indicate 95% confidence intervals. Asterisks indicate statistical significance (*: FDR-adjusted $P < 0.05$; **: $P < 0.01$; ***: $P < 0.001$). BEB: *Basic Endochitinase B* (Solyc10g055800.2), CHI9: *Basic 30 kDa endochitinase CHI9* (Solyc10g055810.2), PR11: *Acidic chitinase PR11* (Solyc05g050130.5), POX51: *peroxidase*, ortholog to *A. thaliana peroxidase 51* (Solyc02g092580.3), NIMIN2: *NIM-interacting 2-like* (Solyc03g119590.1), SAD4: *SAR deficient 4* (Solyc06g036330.1), WRKY40: WRKY40 (Solyc06g068460.3), ERF: *Ethylene Response Factor D3* (Solyc01g108240.4), NBS: *NBS-LRR class*

disease resistance protein (Soly07g056200.3), *Tw1:Tomato Wound Induced 1* (Soly01g107820.2), 23 kDa: *23 kDasubunit of oxygen evolving system of photosystem II* (Soly07g044860.3), *CPK2: calcium-dependent protein kinase*(Soly03g033540.3)

Figure 5: Effect of PA treatment on reactive oxygen species metabolism. **(a)** Percentage of droplets in which DAB staining showed ROS accumulation at one, three, six and 24 hours post treatment. Treatments with different letters are significantly different ($P < 0.05$). Error bars indicate the standard error of the mean. $N = 10$ (ten leaflets per treatment, each with three droplets). **(b)** Peroxidase activity in shoot and root samples of tomato seedlings harvested 14 days after emergence (24 hours after the second PA treatment) and treated with PA or a corresponding control. Error bars indicate the standard error of the mean. ($N = 6$) **(c)** Representative images of PA-treated, DAB-stained leaflets from the experiment shown in Figure 4a. The white arrow shows the location where the PA droplet was applied.

Figure 6: **(a)** PCA plot of samples from tomato roots and shoots harvested after PA or mock treatment (Control), based on the features detected by negative mode UPLC-MS analysis. Shading represent 95% confidence ellipses. **(b)** Heatmap (showing normalized, centered and scaled feature abundances) and hierarchical clustering of samples and features from tomato roots and shoots harvested after PA or mock treatment (Control), based on the same dataset as used for Figure 6a **(c)** Number of galls in the roots of tomato plants 28 days post inoculation with 250 J2 juveniles of *M. incognita* wild type tomato plants (WT) or tomato plants expressing the *NahG* construct (NahG) and pre-treated with 300 μM piperonylic acid (PA) or a corresponding mock treatment (Control). Treatments with different letters differ significantly.

Figure 7: Effect of exposure to a dilution series of crude methanol extracts from PA or mock-treated tomato shoots and roots on the motility of *M. incognita* J2s. **(a)** after 4 hours of exposure **(b)** after 24 hours of exposure. Data are plotted with a logarithmic x-axis. Quasibinomial regression lines, and their associated 95% confidence intervals (shown as shaded bands, are shown).

Figure 8: Primed accumulation of phenylpropanoid pathway-related products in leaves, stems and roots of tomato plants pre-treated with PA or a corresponding mock treatment and subsequently inoculated with 400 *M. incognita* J2 juveniles ('Mi'). Plants were harvested seven days after inoculation. **(a)** Quantity of free phenolic compounds and other reducing substances as determined via the Folin-Ciocalteu assay, expressed in mg gallic acid equivalent per g of fresh weight. **(b)** Quantity of cell-wall bound phenolic compounds and other reducing substances released after sodium hydroxide digestion as determined via the Folin-Ciocalteu reaction, expressed in mg gallic acid equivalent per g of fresh weight. **(c)** Amount of lignin as determined through the acetyl bromide method (expressed as % of total dry cell wall mass). 'ns' (not significant) indicates no differences between treatments in a tissue; where significant differences between treatments exist, letters are used to indicate which treatments differ significantly ($P < 0.05$). $N = 15$.

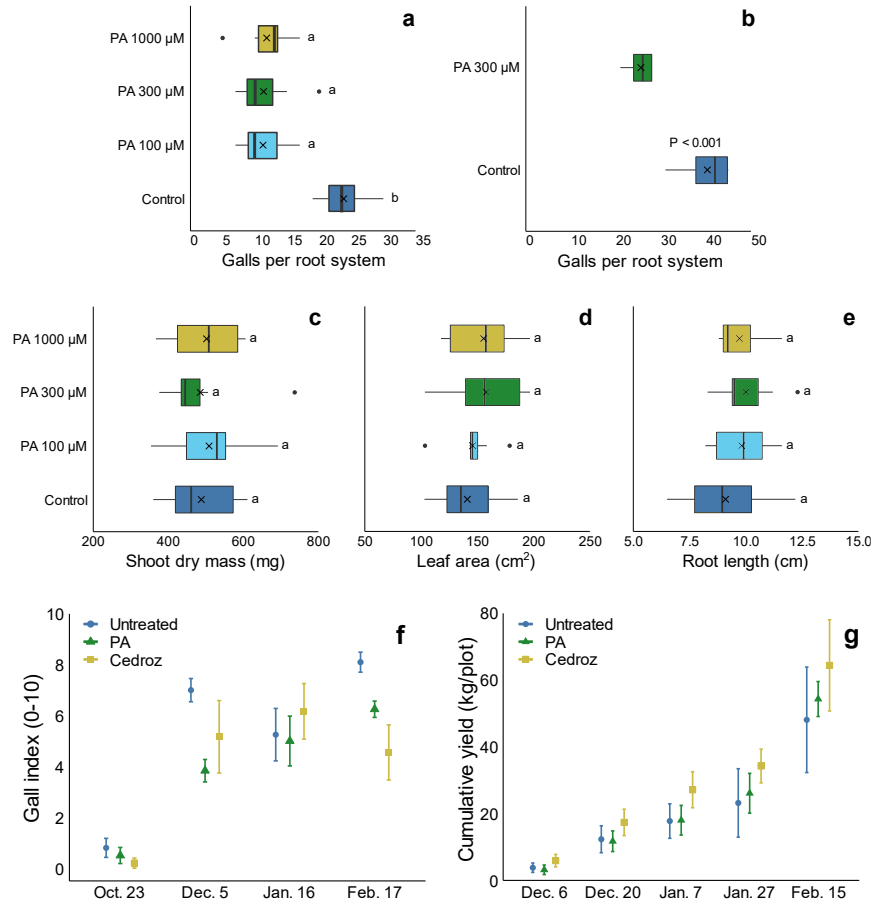


Figure 1: The effects of PA treatment on tomato growth and susceptibility to root-knot nematodes. **(a)** Number of galls in the roots of tomato plants 28 days after inoculation with 250 *M. incognita* J2s. **(b)** Number of galls in the roots of rice plants 14 days after inoculation with 250 *M. graminicola* J2s. **(c-e)** Effect of weekly PA treatment on the dry shoot mass (c), leaf area (b) and root system length (c) of tomato seedlings. Treatments with different letters differ significantly ($P < 0.05$). $N = 8$. **(f-g)** Efficacy of PA (applied three times as a 300 μM foliar spray) at controlling root-knot nematodes in tomato plants grown in soil naturally infested with a mixed population of *M. incognita* and *M. javanica*. Cedroz, a commercial nematicide, was used as reference treatment. PA was applied three times, Cedroz was applied six times according to the manufacturer's instructions. Error bars indicate the standard error of the mean. **(f)** Disease severity (as indicated Zeck's galling index) over the course of the trial. $N = 4$ plots per treatment (from each of which four plants were uprooted and evaluated at the first three time points and ten at the final time point). **(g)** Cumulative yield (in kg tomatoes per plot). $N = 4$ plots per treatment.

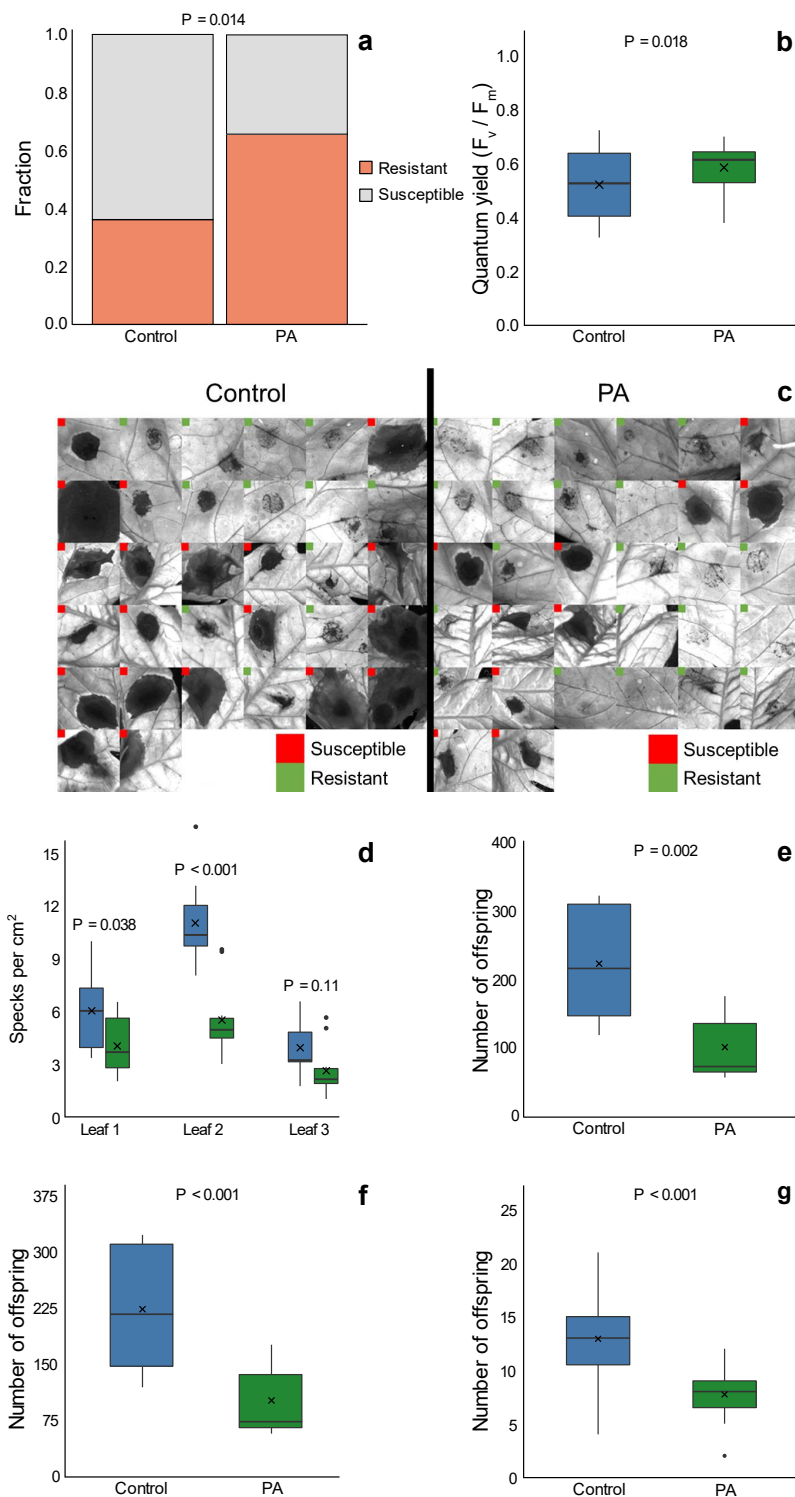


Figure 2: Efficacy of PA against foliar pests and diseases of tomato: *Botrytis cinerea* R16, *Pseudomonas syringae* DC3000, *Tetranychus urticae*, *Aculops lycopersici* and *Frankliniella occidentalis*. **(a)** Percentage of *B. cinerea* inoculation sites that led to successful colonization four days after inoculation (N = 32 inoculation sites on 8 leaves). **(b)** F_v/F_m (photosynthesis quantum yield) in *B. cinerea* infection sites **(c)** chlorophyll images of *B. cinerea* inoculation sites in tomato leaves pre-treated with 300 μ M piperonylic acid (PA) or a corresponding mock treatment (Control) ; black coloration indicates *B. cinerea*-induced necrosis. **(d)** Number of *P. syringae* DC3000 specks per cm² of leaf area five days after dip inoculation (N = 12). **(e)** Number of *T. urticae* offspring present on tomato plants ten days after inoculation with 10 adult females (N = 8). **(f)** Number of *A. lycopersici* offspring present on tomato plants ten days after inoculation with 30 mixed-sex mites

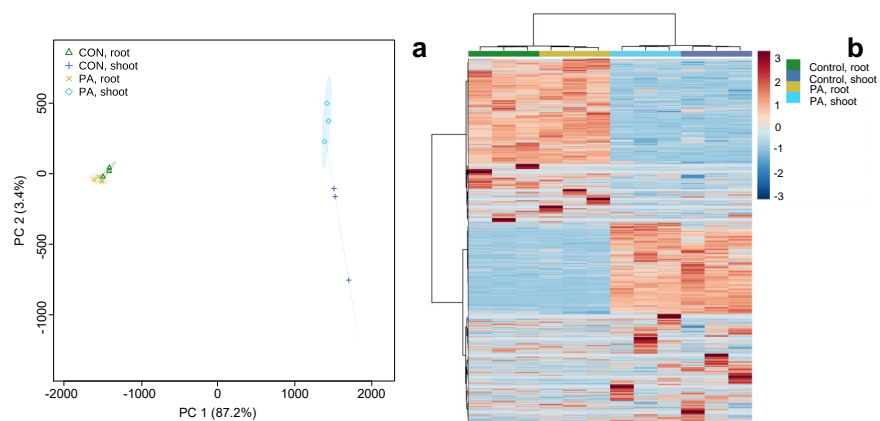


Figure 3: (a) Principal component analysis scatterplot of samples from tomato roots and shoots harvested 24 hours after the second PA or mock treatment (CON), based on mRNA-sequencing based analysis of gene expression. Shaded ellipses represent 95% confidence ellipses. **(b)** Heatmap (showing normalized, centered and scaled expression values) and hierarchical clustering of samples and transcripts from tomato roots and shoots harvested after PA or mock treatment (CON), based on the same dataset as (a).

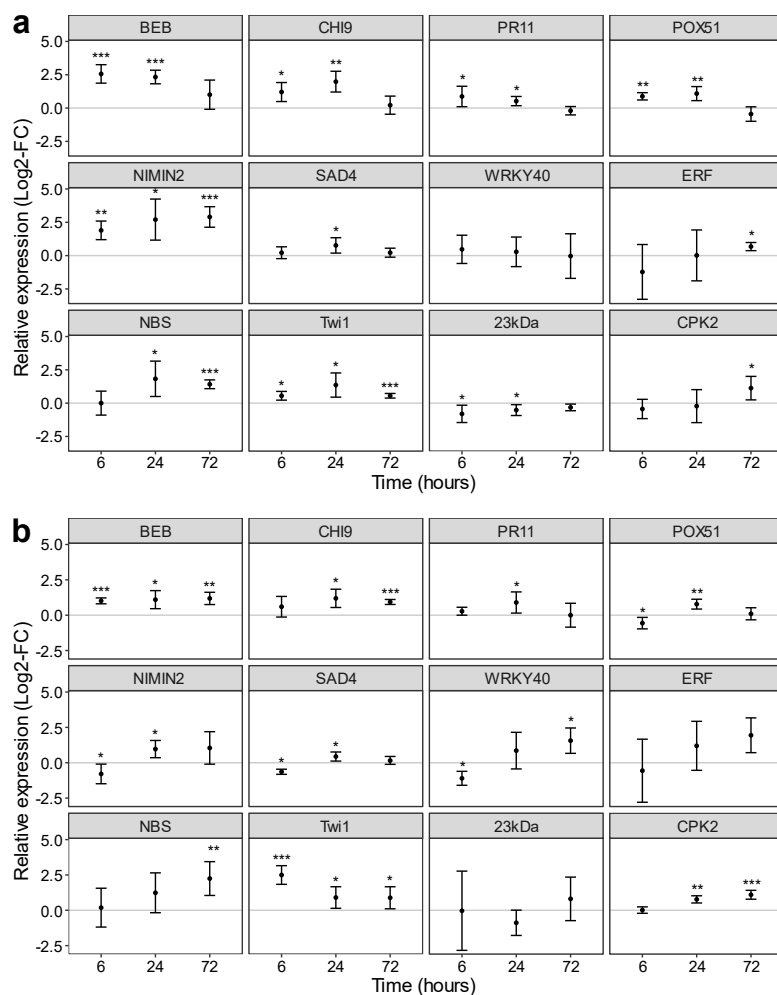


Figure 4: Gene expression in shoots **(a)** and roots **(b)** of tomato seedlings harvested 6, 24 and 72 hours after the second foliar treatment with 300 μ M PA relative to mock-treated control plants. Relative expression values are \log_2 -transformed; error bars indicate 95% confidence intervals. Asterisks indicate statistical significance (*: FDR-adjusted $P < 0.05$; **: $P < 0.01$; ***: $P < 0.001$). BEB: *BASIC ENDOCHITINASE B* (Solyc10g055800.2), CHI9: *BASIC 30 KDA ENDOCHITINASE CHI9* (Solyc10g055810.2), PR11: *ACIDIC CHITINASE PR11* (Solyc05g050130.5), POX51: *PEROXIDASE*, ortholog to *A. thaliana PEROXIDASE 51* (Solyc02g092580.3), NIMIN2: *NIM-INTERACTING 2-LIKE* (Solyc03g119590.1), SAD4: *SAR DEFICIENT 4* (Solyc06g036330.1), WRKY40: *WRKY40* (Solyc06g068460.3), ERF: *ETHYLENE RESPONSE FACTOR D3* (Solyc01g108240.4), NBS: *NBS-LRR CLASS DISEASE RESISTANCE PROTEIN* (Solyc07g056200.3), Twi1: *TOMATO WOUND INDUCED 1* (Solyc01g107820.2), 23 kDa: *23 kDa SUBUNIT OF OXYGEN EVOLVING SYSTEM OF PHOTOSYSTEM II* (Solyc07g044860.3), CPK2: *CALCIUM-DEPENDENT PROTEIN KINASE* (Solyc03g033540.3)

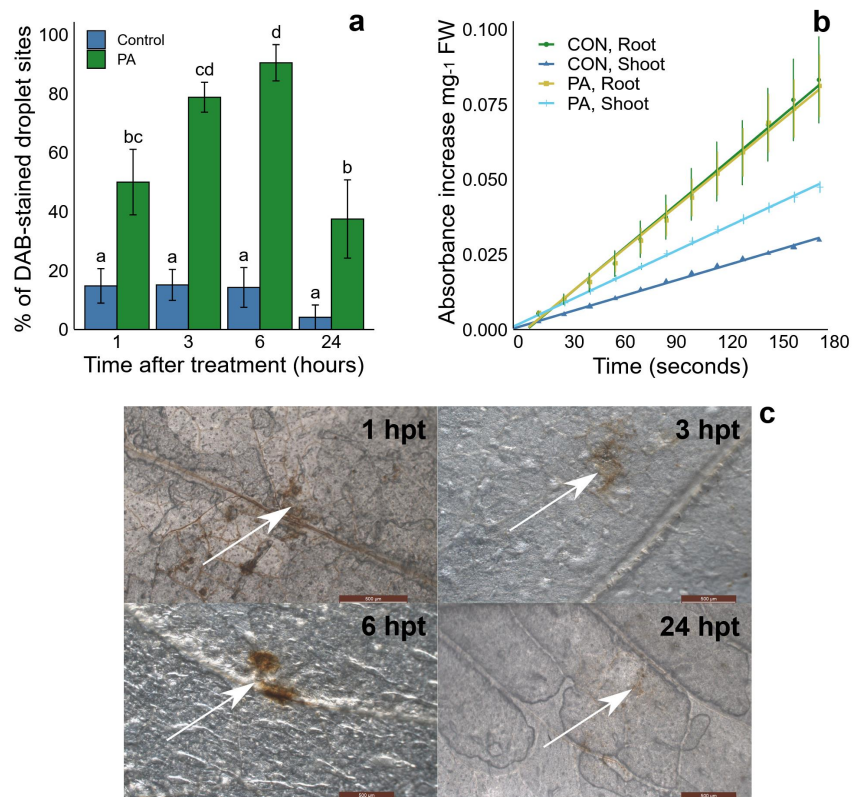


Figure 5: Effect of PA treatment on reactive oxygen species metabolism. **(a)** Percentage of droplets in which DAB staining showed ROS accumulation at one, three, six and 24 hours post treatment. Treatments with different letters are significantly different ($P < 0.05$). Error bars indicate the standard error of the mean. $N = 10$ (ten leaflets per treatment, each with three droplets). **(b)** Peroxidase activity in shoot and root samples of tomato seedlings harvested 14 days after emergence (24 hours after the second PA treatment) and treated with PA or a corresponding control. Error bars indicate the standard error of the mean. ($N = 6$) **(c)** Representative images of PA-treated, DAB-stained leaflets from the experiment shown in Figure 4a. The white arrow shows the location where the PA droplet was applied.

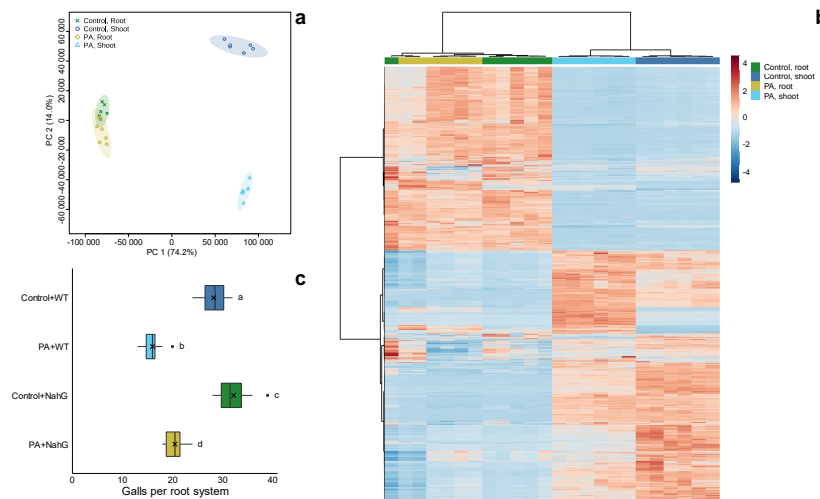


Figure 6: (a) PCA plot of samples from tomato roots and shoots harvested after PA or mock treatment (Control), based on the features detected by negative mode UPLC-MS analysis. Shading represent 95% confidence ellipses. (b) Heatmap (showing normalized, centered and scaled feature abundances) and hierarchical clustering of samples and features from tomato roots and shoots harvested after PA or mock treatment (Control), based on the same dataset as used for Figure 6a (c) Number of galls in the roots of tomato plants 28 days post inoculation with 250 J2 juveniles of *M. incognita* wild type tomato plants (WT) or tomato plants expressing the *NahG* construct (NahG) and pre-treated with 300 μ M piperonylic acid (PA) or a corresponding mock treatment (Control). Treatments with different letters differ significantly.

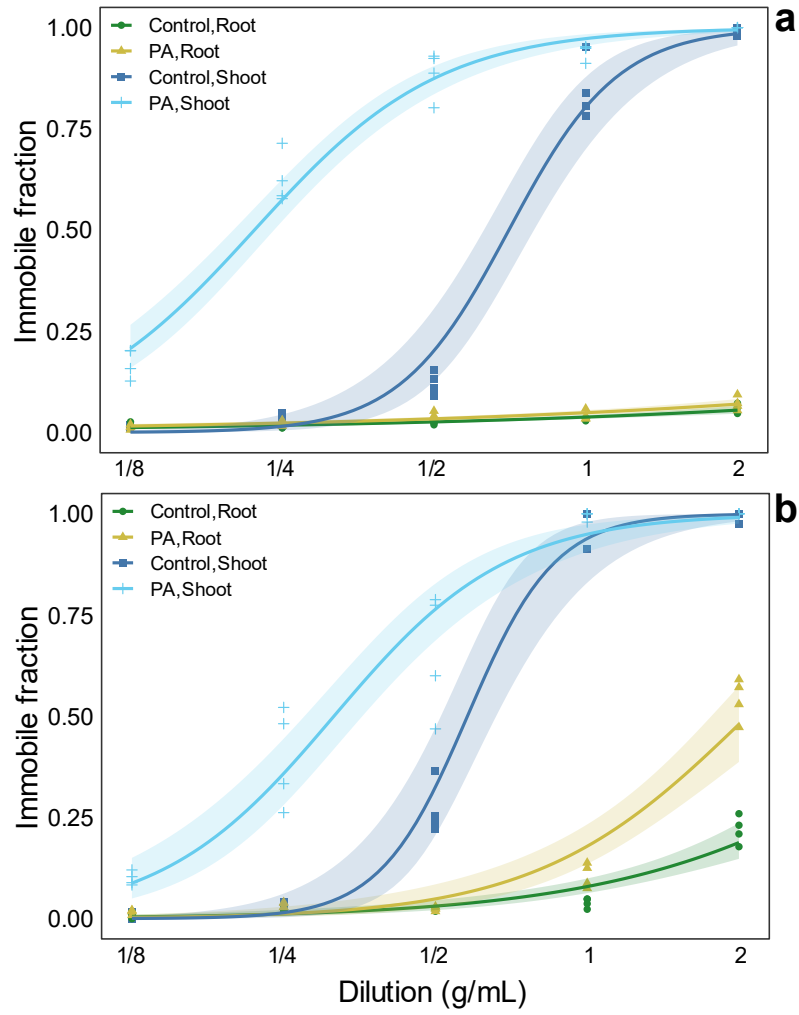


Figure 7: Effect of exposure to a dilution series of crude methanol extracts from PA or mock-treated tomato shoots and roots on the motility of *M. incognita* J2s. (a) after 4 hours of exposure (b) after 24 hours of exposure. Data are plotted with a logarithmic x-axis. Quasibinomial regression lines, and their associated 95% confidence intervals (shown as shaded bands), are shown.

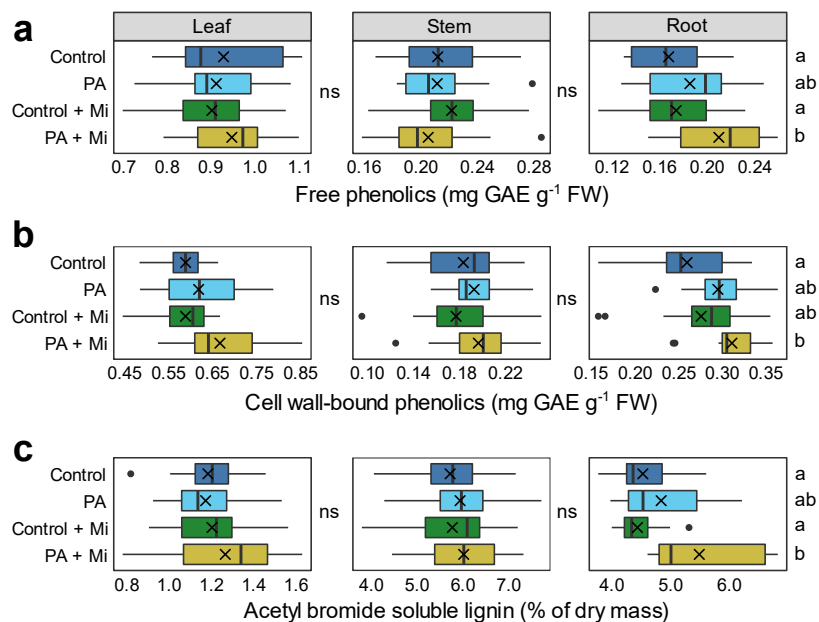


Figure 8: Primed accumulation of phenylpropanoid pathway-related products in leaves, stems and roots of tomato plants pre-treated with PA or a corresponding mock treatment and subsequently inoculated with 400 *M. incognita* J2 juveniles ('Mi'). Plants were harvested seven days after inoculation. **(a)** Quantity of free phenolic compounds and other reducing substances as determined via the Folin-Ciocalteu assay, expressed in mg gallic acid equivalent per g of fresh weight. **(b)** Quantity of cell-wall bound phenolic compounds and other reducing substances released after sodium hydroxide digestion as determined via the Folin-Ciocalteu reaction, expressed in mg gallic acid equivalent per g of fresh weight. **(c)** Amount of lignin as determined through the acetyl bromide method (expressed as % of total dry cell wall mass). 'ns' (not significant) indicates no differences between treatments in a tissue; where significant differences between treatments exist, letters are used to indicate which treatments differ significantly ($P < 0.05$). $N = 15$.